University of Zurich[UZH]

Landscape impacts of catastrophic glacier detachments

GEO 511 Master's Thesis

Author
Jonas Felix Laube
19-059-658

Supervised by
Mylène Jacquemart (jacquemart@vaw.baug.ethz.ch)
Dr. Evan Miles
Dr. Simon Allen

Faculty representative
Prof. Dr. Christian Huggel

02.10.2024
Department of Geography, University of Zurich

University of Zurich[UZH]

ETH zürich

Jonas F. Laube
19-059-658
jonasfelix.laube@uzh.ch

Landscape Impacts of Catastrophic Glacier Detachments

Master's Thesis

Department of Geography
Environment and Climate
University of Zurich

Supervision

Dr. Mylène Jacquemart (ETH & WSL)
Dr. Evan Stewart Miles (WSL & UZH)
Dr. Simon Allen (UZH)

Faculty Member

Prof. Dr. Christian Huggel (UZH)

October 2, 2024

Abstract

Glacier detachment is a recently discovered type of glacier instability in which large parts of a glacier fail catastrophically. The detached glacier ice, in combination with mobilised lithic material, may lead to mudflows further down the valley, leaving a trail of devastation in its wake. Due to the novelty of this high mountain hazard, its medium- and long-term effects on the landscape have been little studied. In this thesis, I address this research gap by analysing the medium-term impacts of glacier detachments in the Degilmoni Poyon and Shuraki Kapali catchments in central Tajikistan using remote sensing imagery.

Between 2016 and 2023, four out of five glaciers in the Degilmoni Poyon and Shuraki Kapali catchments affected by glacier detachments rapidly regained volume, despite above average warm and dry climatic conditions. Consequently, the exposed glacier beds were re-covered by ice within a few years, providing protection against erosion. Just as quickly as the glaciers recovered after the detachments, their deposits in the runout zones vanished. In the Degilmoni Poyon catchment, the deposited ice melted within just three years. Five years after the detachment, only missing patches of vegetation and striations in a few areas of the runout zone indicate that a detachment has occurred.

Glacier detachments also pose a significant risk to communities, as can be seen in the Shuraki Kapali catchment. In both 2016 and 2017, glacier detachments triggered mudflows and flooding in inhabited areas, damaging infrastructure and destroying farmland. Although the affected area has since been avoided for new development, a new settlement has been built in its immediate vicinity. This is a cause for concern, as the new findings suggest that glacier detachments could also occur there in the future.

The findings of this study highlight the transience of the traces left by glacier detachments in the landscape. However, the fact that the traces left by a detachment disappear relatively quickly should not obscure the reality that glacier detachments pose an immediate threat to villages located in their runout zones.

Acknowledgements

This work would not have been possible without the support and contribution of several people, for which I would like to express my gratitude.

For the inspiring meetings, the shared ideas and tips and the guidance in general:
Dr. Mylène Jacquemart, Dr. Evan Stewart Miles and Dr. Simon Allen

For organisational support and feedback on content:
Prof. Dr. Christian Huggel

For proofreading and technical support:
Esther Dällenbach, Leo Hösli, Simon Laube, Katia Soland, Severin Weber

For the provision of data:
Silvan Leinss, Achille Pierre Jouberton

For making my studies and master's thesis an unforgettable time:
My friends and my family

I would also like to acknowledge that I used the Large Language Model 'ChatGPT 3.5' as a help in the process of writing computer code. I also used 'DeepL' to spell check and improve the formulation of texts. However, this work and the results presented in it are not the direct result of artificial intelligence tools.

Contents

1. Introduction

1.1 Context and Problem Statement

On 2 September 2002, large parts of the Kolka glacier in the North Caucasus detached. The huge rock-ice slide that followed involved the mobilisation of about 100×10^6 m^3 of glacier ice and lithic material, which turned into a debris/mud flow further downstream (Haeberli et al. 2004; Kotlyakov, Rototaeva, & Nosenko 2004). As a consequence, more than 120 people were killed, a village was partly inundated and severe infrastructure damage was caused (Haeberli et al. 2004). It was the first time that such an event had been documented and was thought to be unique due to the unusual location of the Kolka glacier. The proximity of a dormant volcano led to the assumption that high geothermal fluxes beneath the glacier were causing additional melting of the bottom of the glacier (Haeberli et al. 2004; Kotlyakov, Rototaeva, & Nosenko 2004). This, combined with increased basal shear and normal stresses due to rock and icefalls on the glacier during the few weeks prior to the Kolka event, has been considered to be the primary cause of the detachment (Evans et al. 2009; Huggel et al. 2005).

14 years later, in 2016, the neighbouring Aru-1 and Aru-2 glaciers in western Tibet collapsed within two months. Nine herders and hundreds of their animals were killed by the ice masses and the resulting debris flow (Kääb et al. 2018). Unlike the Kolka event, there were no known conditions of high geothermal fluxes. This raised the question of whether such events are more frequent than previously thought and led to more research on the causes of such catastrophic events. Since then, several comparable events have been identified, and different terms have been introduced in recent years to describe these sudden, large-volume detachments of high mountain glaciers: glacier slides (Petrakov et al. 2018), glacier collapses (Gilbert et al. 2018; Kääb et al. 2018) and glacier detachments (Evans & Delaney 2015; Jacquemart & Cicoira 2022; Leinss et al. 2021). In this master's thesis, I will use the term 'glacier

detachment' because it is the one that is most commonly used in other scientific publications.
In the last few years, there have been several studies on the causes of glacier detachments (e.g. Jacquemart et al. 2020; Kääb et al. 2018, 2021; Zou et al. 2023), but to date, there has been very little research on the impacts of glacier detachments on the alpine landscape. Only two works investigated specifically the landscape impacts of glacier detachments: Jacquemart and Cicoira (2022) examined the geomorphic and sedimentary signatures of the Flat Creek glacier detachment in Alaska. Kääb and Girod (2023) focused on the bed erosion following the glacier detachment of Sedongpu Glacier in Tibet. Most other papers on glacier detachments focus on the period starting before a glacier detachment until shortly after. My thesis, however, focuses on the period shortly after the event until 2023.
The goal of this master's thesis is to contribute to a better understanding of the medium-term effects of glacier detachments on the landscape by studying the Degilmoni Poyon (DP) and the Shuraki Kapali (SK) catchments in the Petra Pervogo range (Tajikistan). These two catchments are of particular interest because they have experienced one or more glacier detachments in the last decade, some of which have directly affected downstream settlements (Leinss et al. 2021). Furthermore, extensive data for these two catchments has been acquired through the Pamir Project (cf. section 2.2), which is an indispensable precondition for such work.

1.2 Relevance

To date, very little is known about the response of the alpine landscape after a glacier detachment. This is not surprising given the recent nature of most documented events. By 2021, there was still not a single study that focused specifically on the landscape impacts of glacier detachments (Jacquemart & Cicoira 2022). Since then, two studies on the responses of alpine landscapes have been published, but have also shown that further research is needed. Jacquemart et al. (2022) examined the geomorphic and sedimentary signatures of the Flat Creek glacier detachment in Alaska. They found that a careful interpretation of all available geomorphological and sedimentological evidence, interpreted in the context of the landscape, can reveal the origin of a glacier detachment deposit. At the same time, Jacquemart et al. (2022) also stated that further investigations of other contemporary glacier detachments are necessary to solidify and generalise the understanding of these deposits. Kääb and Girod (2023) identified impressive erosion rates of 30 meters per month

from June to August 2021 in the exposed area following the glacier detachment of the Sendogpu glacier in Tibet. However, how the erosion rate in the Sendogpu glacier forefield compares with those of other catchments influenced by glacier detachments has not yet been fully clarified, as Kääb and Girod (2023) have not systematically investigated these. Apart from the two mentioned above, the lack of studies on the landscape impacts of glacier detachments reveals a major research gap. A better understanding of this young field of research is needed for several reasons.

It is important to know what traces a glacier's collapse leaves in the landscape and how long they last. This allows us to find out whether and when glacier collapses have occurred in other places and to understand the frequency of past events. The more glacier detachments are documented, the more data can be collected to improve our understanding of their causes and how they behave in different climatic and topographic settings. This knowledge is crucial for identifying glaciers that are prone to detachment and can, therefore, be important for effective natural hazard management in populated regions or areas with critical infrastructure.

It is assumed that climate change will affect the frequency of future glacier detachments around the world through a variety of different factors. As the glacier geometry adapts to an increase in temperature, it may shift into or out of a state in which glacier detachments are possible (Kääb et al. 2021). Climate change affects various preconditions and possible triggers for glacier detachments (cf. section 2.3). Rising temperatures will increase meltwater input, more frequent heavy precipitation events will lead to high water availability in a short period of time, while drier summers will limit water availability (Calvin et al. 2023). However, the question of whether detachments will become more frequent due to climate change has not yet been answered (Jacquemart & Cicoira 2022). It is equally important to understand whether climate change will increase the frequency of glacier detachments as it is to know whether a particular glacier will be able to regrow after a detachment under current and future climate conditions. There are no studies on this either, even though this topic is highly relevant for assessing the danger posed by glaciers that have lost a large volume due to detachment.

1.3 Objectives and Research Questions

This master's thesis is part of the Pamir Project, aiming to improve our understanding of climate change impacts on the high-mountain environments of Central Asia (cf. section 2.2). Specifically, this thesis expands the knowledge of the medium-term

response of alpine landscapes to glacier detachments, which is relevant beyond the Pamir Mountains. In the context of this thesis, I will focus on the Degilmoni Poyon and Shuraki Kapali catchments in the Petra Pervogo Range in central Tajikistan. The first goal is to find out what processes are taking place in areas exposed by glacier detachments and whether glacier regrowth or erosion can be observed. The findings of this thesis allow to assess whether more detachments in the Degilmoni Poyon and Shuraki Kapali catchments are possible in the future. Additionally, they can be compared with the high erosion rates measured in the exposed area of the Sendogpu glacier (Kääb & Girod 2023). A second goal of this work is to investigate where the detached material is deposited and how it develops over time. Because there has only been one detachment in the Degilmoni Poyon catchment in recent years, and not many different overlapping detachments as in the Shuraki Kapali catchment, these investigations are being carried out in the Degilmoni Poyon catchment. A third goal of this work is to analyse the impact of glacier detachments on inhabited and human-used areas. This includes an analysis of the damage caused by glacier detachments and one of the adaptation measures taken to better protect settlements against further events. As impacts on inhabited areas have only been documented in the Shuraki Kapali catchment in recent years (Leinss et al. 2021), the analysis is limited to this catchment. Based on those three goals, the following research questions were formulated:

- How do glaciers and exposed glacier beds evolve after catastrophic glacier detachments?
- What traces does a glacier detachment leave in its runout zone and how long do they remain visible?
- What are the impacts of glacier detachments on anthropogenic landscapes, and what adaptation measures are being taken to counteract them?

In order to answer the research questions, I used mainly remote sensing imagery. No in-situ data was available, nor was it possible for me to carry out fieldwork as part of this Master's thesis. However, by combining digital elevation models (DEM) with satellite imagery, I was able to identify medium- and large-scale changes in the landscape. For the quantification of elevation and volume changes, I created DEM differences based on different DEM pairs. Satellite images were used for two different purposes. First, I used them to make qualitative assessments of the landscape impacts of glacier detachments. Second, I used them to determine the timing of events, such as detachments and rockfalls. To place the new findings in

a regional context, I determined the mass balance of seven glaciers not affected by detachments in recent years. I additionally analysed the climatic changes in the high mountain areas of central Tajikistan using meteorological data from 1970 to 2022.

2. Background

This chapter provides background information for a better understanding and contextualisation of the work. The first section summarises the state of the art on the three hazardous glacier instabilities 'surging glaciers', 'ice avalanches' and 'glacier detachments'. The Pamir Project, of which this thesis is a part, is described in the second section.

2.1 Hazardous Glacier Instabilities

Recent work has classified glacier detachments as a third type of hazardous glacier instability alongside ice avalanches and glacier surges (Kääb et al. 2021). The next three sections describe the characteristics of these three hazardous glacier instabilities and their differences and similarities.

2.1.1 Surging Glaciers

Surging glaciers alternate between quiescent and surge phases. During the quiescent phase, ice accumulates in the upper reaches of the glacier (Jacquemart & Cicoira 2022). The subsequent surge phase is characterised by a large-scale ice displacement, which occurs at speeds that are 10 to 100 (or more) times faster than the normal flow rate of the glacier (Post 1969). Surges occur periodically (every 15-100+ years) and can result in a glacier advance of up to several kilometres, posing a threat to downstream infrastructure and populations (Jacquemart & Cicoira 2022; Meier & Post 1969; Steiner et al. 2018). During their surge phase, glaciers have chaotically fractured surfaces, sheared margins and large vertical and horizontal ice displacements (Post 1969). The driving mechanisms behind glacier surges, their frequency and its relation to climate are still not fully understood (Jacquemart & Cicoira 2022; Steiner et al. 2018). Various theories have been proposed to explain the behaviour of surging glaciers, such as till deformation, changes in the subglacial drainage system and a 'thermal switch', but none of these can explain the full range of surging glaciers

observed (Jacquemart & Cicoira 2022). Statistically, surging glaciers are larger in area and longer than average glaciers (Sevestre & Benn 2015), but glacier advance distances are not related to the original length of the glacier (Goerlich, Bolch, & Paul 2020). Surging glaciers are found in high mountain regions around the world, but tend to be clustered in particular regions (Harrison & Post 2003; Sevestre & Benn 2015). One such cluster happens to be in the Pamir Mountains, where 186 out of approximately 13'500 glaciers have been identified as surging glaciers (Goerlich, Bolch, & Paul 2020).

2.1.2 Ice Avalanches

Ice avalanches originate from steep glaciers and are the result of ice falling and sliding down-slope under the influence of gravity (Alean 1985). The ice stops when its kinetic energy is completely destroyed by frictional forces (Alean 1985). Pralong and Funk (2006) created a classification of ice avalanches based on the glacier geometry (balanced and unbalanced), the bedrock geometry (ramp and terrace) and the failure mode (slab fracture and wedge fracture). Balanced glaciers are typically temperate glaciers where the accumulation in the upper part of the glacier is compensated by ablation in the lower part, resulting in a balanced steady state. In contrast to temperate glaciers, cold-based glaciers are unable to slide over their bed and, therefore, lose ice primarily through ice break offs. The largest ice avalanches are expected to occur on glaciers with a constant inclination, defined by Pralong and Funk (2006) as ramp glaciers (Jacquemart & Cicoira 2022). Smaller but more frequent ice avalanches can be anticipated from terrace glaciers, where the bedrock slope steepens abruptly (Jacquemart & Cicoira 2022; Pralong & Funk 2006). In addition to the bedrock geometry, the failure mode also has an important influence on the volume of the ice avalanches. Slab fractures produce ice avalanches with volumes of $10^5 - 10^6$ m^3, whereas wedge fractures typically produce volumes in the range of $10^3 - 10^5$ m^3 (Pralong & Funk 2006). One of the largest documented ice avalanches occurred on the Altelsgletscher in 1895 with a volume of about 3.8×10^6 m^3 (Du Pasquier 1896). It was the result of a slab failure on a ramp glacier. The ice avalanche caused six deaths and about forty dead cows (Du Pasquier 1896). Even today, it is difficult to detect hazardous situations for avalanching glaciers, as the destabilisation processes can only be observed indirectly through geometrical changes, crevasse formation and velocity increase (Pralong & Funk 2006).

2.1.3 Glacier Detachments

Glacier detachments are characterised by a low slope angle of 10-20° of their originating glacier, their large volume of millions to tens of millions of cubic meters of ice and lithic material as well as their long runout distances (Jacquemart & Cicoira 2022; Kääb et al. 2021). Glacier detachments are less common than ice avalanches and surging glaciers, but the high mobility combined with the large volumes can pose a serious threat to communities and settlements in the runout zone (Kääb et al. 2021). Although being a distinct type of hazardous glacier instability, glacier detachments combine elements of both glacier surges and ice avalanches from steep glaciers. As with surging glaciers, the glacier adjusts its geometry in response to stress changes in a surge-like process that propagates an initial instability through large parts of the glacier. As with ice avalanches, the glacier is not able to adjust continuously (Kääb et al. 2021). Glacier detachments are even discussed to be a catastrophic endmember of the surging process (Kääb et al. 2018) or a specific kind of glacier surge in which the force balance cannot be achieved by longitudinal and lateral stresses when basal friction is suddenly reduced (Kääb et al. 2021).
Despite some similarities, there are also some key characteristics that distinguish glacier detachments from surging glaciers and ice avalanches. Glacier surges differ from glacier detachments primarily in their unusually high ice-flow velocities of up to tens of metres per day over large parts of a glacier for weeks to several years. Another difference between surges and glacier detachments is that the bed of surging glaciers does not fail catastrophically (Kääb et al. 2021). Ice avalanches, on the other hand, originate from steep hanging glaciers and have a shorter runout distance and a smaller volume than glacier detachments (Evans & Delaney 2015; Jacquemart & Cicoira 2022).
The increasing number of documented glacier detachments in recent years is thought to be the result of an observational bias caused by the increasing availability and resolution of satellite imagery (Leinss et al. 2021). To date, about 20 glacier detachments have been recorded at 13 different locations in the Himalayas, the Andes, Alaska and the Caucasus (Kääb et al. 2021). Although the documented glacier detachments occurred in different mountain ranges around the world, there are some clear similarities regarding their location and timing. All but one of the recorded events happened in close proximity to surging type glaciers. Most glacier detachments occurred during the local spring and summer in years with annual air temperatures above average (Kääb et al. 2021; Leinss et al. 2021). Weak bedrock and/or the presence of soft and highly erodible sediments in the area exposed by the de-

tachment were noted for most of the documented glacier detachments (Kääb et al. 2021; Leinss et al. 2021). With one exception, all of the glacier tongues are located in areas where permafrost is suspected to be present, but none of the glacier detachments seems to have occurred at a cold-based glacier where the glacier is completely frozen to its bed (Kääb et al. 2021). The causes of glacier detachments are not yet fully understood, but it is fairly certain that they are a consequence of an extreme reduction in basal resistance caused by unusually high water input from melt and rain (Jacquemart & Cicoira 2022; Kääb et al. 2018).

2.2 Pamir Project

The Pamir Project is an interdisciplinary research project of the Swiss Federal Institute for Forest, Snow and Landscape Research (WSL) and the University of Fribourg (Pamir Project 2022). It has been selected by the Swiss Polar Institute as one of two flagship initiatives for the period 2022-2025. The project addresses the lack of understanding of climate-induced environmental change in the high mountain regions of Asia, the so-called 'Third Pole', and, in particular, the Pamir Mountains. For other regions of the world, such as the Antarctic and the Arctic, the impact of climate change is much better understood to date. This is surprising, given the importance of the Pamir cryosphere to millions of people living in the lowlands. The snow, glaciers and permafrost of the Pamirs are an important source of water for the arid regions stretching to the Aral Sea and play a key role in agriculture and energy production.

Some glaciers in the Pamir Mountains are retreating, but there are also healthy glaciers. For this unique state of the glaciers, there are three hypotheses. The first is a decrease in summer temperatures due to a change in the monsoon. The second is an increase in winter and spring precipitation due to interactions between the monsoon and the westerlies. The third hypothesis is that evapotranspiration over the vast irrigated agricultural areas of the Pamir-Karakorum region of Pakistan creates a moist air mass that is transported to the high altitudes of the Pamirs, where it precipitates as snow. However, none of these hypotheses has been tested using direct measurements. This research gap will be addressed by an improved environmental monitoring network in different catchments across the Pamirs, in collaboration with local partners. In order to get a holistic picture of the Pamir cryosphere, the project is divided into six clusters, of which my master's thesis can be assigned to cluster number 5:

1. Climate and Environmental History
2. Mountain Permafrost
3. Glaciers, Snow and Hydrology
4. Microbial Biochemistry
5. Cryospheric Hazards
6. History of Glacier Science

By linking the research of these clusters, it will be possible to answer important questions about the Pamir cryosphere: How are the cryosphere and its ecosystems responding to climate change? Why are some glaciers healthy and others retreating? What is the extent of additional water availability due to permafrost thaw? Knowing the answers to these questions will provide a better understanding of this important headwater region, which is crucial for developing improved future runoff forecasts and hazard assessments.

2.3 DEM Differencing

Quantitative monitoring of the evolution of the Earth's surface in a variety of environments and at a range of spatial scales and temporal frequencies is a key aspect of geomorphological research (Williams 2012). A widely used method for quantifying volume change is DEM differencing. The term DEM refers to a digital representation of the elevations of a topographic surface in the form of a georectified point or area-based grid covering the Earth or other solid celestial bodies (Guth et al. 2021). Differencing such DEMs is done by subtracting the elevations of an older DEM from the elevations of a newer DEM, cell by cell. The resulting DEM difference provides a high-resolution, spatially distributed surface model of topographic and volumetric change over time (James et al. 2012).
Due to the above mentioned properties, DEM differencing is a widely used method in a variety of research areas dealing with changes on the Earth's surface. The following selection of specific applications of DEM differencing is intended to illustrate its widespread use and wide range of possible applications. DEM differencing has been used to determine glacier mass balances in Central Asia (Barandun et al. 2021), to determine the volume eroded by a landslide in Slovakia (Prokešová et al. 2014), and to study topographic changes due to lava flows (Kubanek, Poland, & Biggs

2021). It has also been used to study geomorphic changes due to glacial outburst floods in Chile (Jacquet et al. 2017), to assess sediment denudation rates in Taiwan (Kumar et al. 2024), and to map snow depth in remote mountainous areas (Marti et al. 2016).

3. Study Site

In the context of this work, the two catchments Degilmoni Poyon and Shuraki Kapali are investigated. Theses catchments are situated on the northern slope of the Petra Pervogo range, also known as Peter the First Range or Peter the Great Range, in central Tajikistan (Figure 3.1). The Petra Pervogo range runs roughly west to east and is a foothill of the Pamir Mountains. Both the Degilmoni Poyon and the Shuraki Kapali catchment drain into the Surkhob river and are composed of redstone, aleurolite, claystone, conglomerate and limestone (Leinss et al. 2021). The widespread presence of soft lithologies is supported by prominent erosional features and thick glacial debris cover (Leinss et al. 2021). According to a global permafrost map, there is patchy permafrost in the Petra Pervogo range (Obu et al. 2019). The prevailing climatic conditions in the high mountains of central Tajikistan are discussed in detail in Section 6.1.1.
The two catchments are ideal for studying the medium-term landscape impacts of glacier detachments because of three main factors. First, both catchments have experienced glacier detachments in recent years. Second, there is good availability of DEMs and satellite imagery. Third, the importance of a better understanding of glacier detachments and their impacts is highlighted by the presence of inhabited areas further downstream, some of which have been affected in the past.

3.1 Degilmoni Poyon Catchment

The Degilmoni Poyon catchment has an area of about 25 km^2 and extends from 4710 m a.s.l. (above sea level, henceforth assumed) to 1420 m. Within the catchment area is Ghulomon, a small village and a glacier (0.63 km^2) about 9 km upstream of the settlement. The glacier extends from 4400 m to 2850 m and can be divided into two parts. The upper part is located in a steep and rocky area and the lower part is located in a valley with a much lower slope. The two areas are connected by a narrow glacier band that runs down a steep rock face. In 2019, the lower part of this

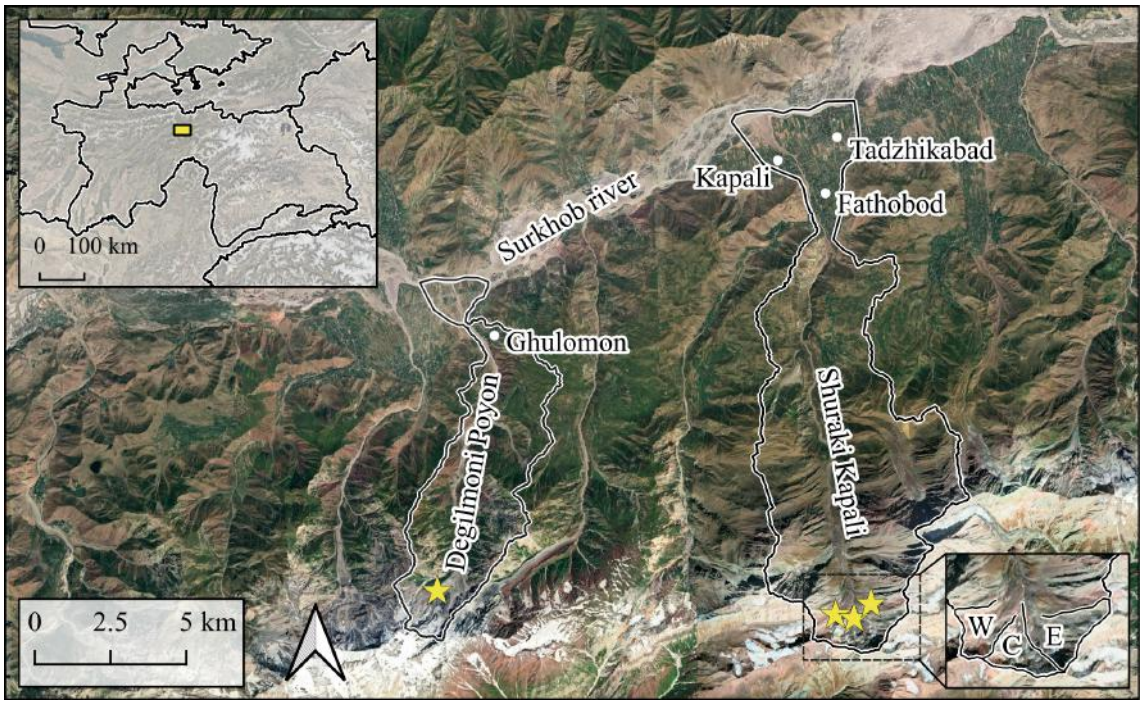

Figure 3.1: Overview map showing the location of the two study catchments and the villages located within them. The yellow stars indicate the location of documented glacier detachments. The small window on the bottom right shows the position of the western (W), central (C) and eastern (E) subcatchments. © Google, Maxar Technologies.

glacier detached, resulting in a debris flow that travelled 6.7 km down the valley, but stopped before reaching the village of Ghulomon (Leinss et al. 2021). Prior to the detachment, the glacier showed surging-like behaviour, advancing 230 m between 1991 and 1995. Apart from the 2019 event, there are no other known detachments or ice avalanches in the Degilmoni Poyon catchment. However, erosion patterns and patches of missing vegetation in the runout zone that are very similar to those of the 2019 event can be seen in satellite imagery prior to 2019 (Leinss et al. 2021).

3.2 Shuraki Kapali Catchment

The Shuraki Kapali catchment is more than twice the size of the Degilmoni Poyon catchment with an area of about 59 km^2, and extends from 4730 m to 1510 m. The three villages of Fathobod, Tadzhikabad and Kapali are located along the lower reaches of the Shuraki Kapali River. The Randolph Glacier Inventory 7.0 (RGI 7.0 Consortium 2023) lists a total of twelve glaciers in the Shuraki Kapali catchment, including glaciers located in tributary catchments that drain into the Shuraki Kapali

river. This study focuses on four of these glaciers (0.09-0.43 km^2), which are located in the southernmost part of the Shuraki Kapali catchment between 4000 m and 3300 m and can be divided into three subcatchments (3.1). There are two glaciers in the western subcatchment and one each in the central and eastern subcatchments. A closer look reveals that the actual contours of these glaciers are quite different from those shown in the Randolph Glacier Inventory. This is because the three subcatchment areas are a hotspot for glacier detachments and ice avalanches, which lead to regular changes in the glacier contours. Six glacier detachments and four rock-ice avalanches have been documented for the three subcatchments between 1973 and 2019 (Leinss et al. 2021). On 28 August 2016, a glacier detachment occurred in the western subcatchment, which led to a mudflow and caused infrastructural damage in the villages of Kapali and Fathobod. The largest detachment in recent years occurred on 10/11 July 2017 in the western subcatchment, when almost the entire glacier detached with an area of about 250×10^3 m^2 (Leinss et al. 2021).

4. Data

I used mainly remote sensing imagery to analyse the landscape impacts of glacier detachments in the Degilmoni Poyon and Shuraki Kapali catchments. There was no in-situ data available, nor was it possible for me to carry out any field work as part of this Master's thesis. However, by combining digital elevation models with satellite imagery, I was able to identify medium and large scale landscape changes. In addition to the remote sensing imagery, I used a meteorological dataset to analyse the climatic conditions in the high mountain regions of central Tajikistan and how they have changed since 1970.

4.1 Digital Elevation Models

For the creation of DEM differences I used DEMs of three different satellite missions, namely Pléiades, WorldView and TanDEM-X. All the different DEMs and their acquisition dates used for this work are listed in the Table 4.1.
Both Pléiades and WorldView DEMs have a horizontal resolution of 2 m, while TanDEM-X has a horizontal resolution of about 12 m. An assessment of the vertical accuracy of the global TanDEM-X DEM in a mountainous environment showed a significant decrease in accuracy with increasing slope. In areas with a slope of less than 10°, the vertical accuracy is around 5 m, rising to over 10 m in areas with a slope of more than 50°(Gdulová, Marešová, & Moudrý 2020). Unfortunately, such detailed analyses of the vertical accuracy of WorldView and Pléiades DEMs are not available. However, it can be assumed that their vertical accuracy also decreases with increasing slope, as studies on other DEMs, such as ASTER and SRTM DEMs, have also shown that the accuracy in steep terrain is significantly lower than in flat regions (Mukherjee et al. 2012).
With two exceptions, the DEMs used in this thesis were acquired at a time when there was no or only a very thin snow cover above 3500 m in the Petra Pervogo range. One of the exceptions is the TanDEM-X DEM from 05.09.-29.10.2014. During the

first satellite flyover, the Petra Pervogo range was free of snow, as can be seen in the Landsat-8 image of 6 September 2014. However, the Landsat-8 image of 24 October 2014 shows a snow cover above 2800 m, which was probably still present during the second flyover 5 days later. As the penetration depth of the X-band SAR signal is between 3 and 7 m in dry snow areas (Zhao & Floricioiu 2017), the observed snow cover should not have a strong influence on the DEM from 05.09.-29.10.2014 and therefore will not affect the subsequent co-registration.
When the WorldView DEM of 10 April 2020 was acquired, areas above 2800 m on north-facing and above 3000 m on south-facing slopes were snow-covered, as can be seen in the Sentinel-2 image of 18 April 2020. Due to the acquisition date in spring, it is likely that there are still areas in higher elevations with snow depths of several meters, particularly on northern slopes and in depressions where snow is accumulated by avalanches and wind drift (which is true for most of the exposed areas studied). Combined with the fact that spring snow is often significantly wetter than fresh snow, which reduces the penetration depth of electromagnetic waves (Casey et al. 2016), it is very likely that the observed snow cover has an impact on the vertical DEM accuracy.
In addition to snow cover, there are two other factors that affect the accuracy of some of the DEMs. The Pléiades DEMs have small areas of no data, which occur mainly in steep areas on south-facing slopes. The 2019 WorldView DEM shows some artefacts resulting from the DEM generation process. In addition, the DEM contains clouds that cover some areas within the exposed area and the surrounding slopes in the Degilmoni Poyon catchment.

Table 4.1: List of all DEMs used.

Acquisition date or period	DEM name	Resolution	Source
05.09.2014 - 29.10.2014	TanDEM-X	12m	Leinss (2023)
09.09.2018	WorldView	2m	Jacquemart Mylène (2023)
03.08.2019	WorldView	2m	Jacquemart Mylène (2023)
10.04.2020	WorldView	2m	Jacquemart Mylène (2023)
04.09.2022	Pléiades	2m	Miles (2023)
03.09.2023	Pléiades	2m	Miles (2023)

4.2 Satellite Images

For a qualitative analysis of landscape changes I used a variety of satellite imagery, including Landsat-8 (30 m vertical resolution) and Sentinel-2 imagery (10 m) as well as high-resolution imagery from Pléiades (2 m), Google Earth Pro (<0.5 m) and ESRI World Imagery Wayback (<0.5 m). Sentinel-2 images have a very high temporal resolution, making them useful for determining the timing of events such as detachments and rockfalls. Since Sentinel-2 was only launched in June 2015 (Phiri et al. 2020), I used Landsat-8 imagery for determining the timing of events before summer 2015. High-resolution imagery, such as Pléiades imagery or imagery available on Google Earth Pro and ESRI World Imagery Wayback, has a lower temporal resolution but a higher spatial resolution. I used these high-resolution images to identify medium-scale features in the landscape, such as crevasses, river courses and houses. I also used the high-resolution imagery to make broad statements about the materials involved in certain processes (e.g. distinguishing between snow/ice and lithic material).

4.3 Meteorological Data

In order to estimate the climatic changes in high-mountain areas of central tajikistan over the last few decades, and to see how the years between 2014 and 2023 compare to the long-term averages, I needed meteorological data. Since no data were available from a meteostation within the Petra Pervogo range itself, I used downscaled and bias-corrected data for a meteostation in the Jiragol district of Tajikistan. The meteostation (39.11507°N, 71.41184°E) is located 1 km north of the Kyzylsu glacier snout and about 65 km east of the Degilmoni Poyon catchment and 50 km east of the Shuraki Kapali catchment. Like the glaciers in the two catchments studied, the meteostation is located on the northern slope of a mountain range in a high-mountain environment (3369 m). Despite the relatively large distance between the meteostation and the study areas, it therefore seems reasonable to use this data set to make rough statements about their climatic conditions. This dataset was prepared by (Jouberton 2024) and contains hourly multi-variable data between 1 January 1970 and 30 September 2023. For my analyses I have limited myself to the two variables temperature and precipitation.

5. Methods

This chapter describes how I quantified volumetric landscape changes using Digital Elevation Models and how I analysed meteorological data. Furthermore, it is explained in detail why I chose different methods when analysing the two catchments.

5.1 Digital Elevation Model Processing

In order to detect and quantify volume changes in the landscape I created several DEM differences (Table 5.1) based on the DEMs listed in the Table 4.1. There are three types of biases that need to be considered when creating a DEM difference (Nuth & Kääb 2011):

1. bias due to the geo-location of the data (x, y and z matrices)
2. elevation dependent bias
3. biases related to the acquisition geometry of the data

Nuth and Kääb (2011) presented methods, which I largely followed, for dealing with these biases and obtaining accurate DEM differences. The following three sections show in detail, the methods I used to generate DEM differences and deal with the biases.

5.1.1 DEM Co-Registration and Differencing

DEM differencing is a process in which two DEMs with different acquisition dates are subtracted from each other, cell by cell. This makes it possible to detect changes in the landscape over time and to determine the position and volume of these changes. For the differencing process to work properly, it is essential that the two DEMs are properly aligned. This means that the two DEMs are not tilted with respect to each other and that there is no vertical or horizontal shift between them. This requires a so-called co-registration of the DEMs.

Table 5.1: List of all DEM differences created.

DEM difference	Reference DEM	Aligned DEM	Coverage
DP-14/20	10.04.2020, WorldView	05.09-29.10.2014, TanDEM-X	DP (partly)
DP-14/23	03.09.2023, Pléiades	05.09-29.10.2014, TanDEM-X	DP (partly)
DP-18/19	03.08.2019, WorldView	09.09.2018, WorldView	DP (partly)
DP-18/23	03.09.2023, Pléiades	09.09.2018, WorldView	DP (partly)
DP-19/22	04.09.2022, Pléiades	03.08.2019, WorldView	DP (partly)
DP-19/23	03.09.2023, Pléiades	03.08.2019, WorldView	DP (partly)
DP-20/22	04.09.2022, Pléiades	10.04.2020, WorldView	DP
DP-22/23	03.09.2023, Pléiades	04.09.2022, Pléiades	DP
SK-14/22	04.09.2022, Pléiades	05.09-29.10.2014, TanDEM-X	SK
SK-14/23	03.09.2023, Pléiades	05.09-29.10.2014, TanDEM-X	SK
SK-22/23	03.09.2023, Pléiades	04.09.2022, Pléiades	SK

Prior to co-registering the DEM pairs, I masked all the erroneous and unstable areas in the reference DEM to ensure that co-registration was not performed over changing surfaces. Erroneous areas are those where the surface elevations in the DEM do not correspond to actual elevation of the terrain due to artefacts or clouds. Unstable areas are those where the landscape is expected to change naturally during the study period. Such areas may include glaciers, steep slopes with ongoing mass movements, regions of high erosion or deposition, and inhabited and cultivated areas.
I did the co-registration of different DEM pairs using the open-source Python package xDEM, which is specifically designed for DEM analysis (Mannerfelt, Hugonnet, & Dehecq 2021). Within xDEM, I used the Nuth-Kääb approach to co-register the DEM pairs (Nuth & Kääb 2011). This approach is named after the paper that first described this method and can be used to reduce horizontal and vertical shifts (Mannerfelt, Hugonnet, & Dehecq 2021). The Nuth-Kääb approach takes advantage of the fact that two non-perfectly aligned DEMs of the same area have a characteristic relationship between the elevation differences and the direction of the terrain (aspect), which relates exactly to the x-y-shift vector between them (Paul et al. 2015). This shift is minimised iteratively until the offset threshold falls below 0.1 m or the maximum number of iterations is reached (500). After aligning the DEMs, I differentiated them also using xDEM.

5.1.2 Elevation and Aspect Dependent Bias Correction

The distribution of the ground control points (GCP) for the DEM generation process is crucial for a good result. If the GCPs are unevenly distributed in the three

dimensions, this can lead to an elevation dependent bias in the resulting DEM, which needs to be corrected for further applications (Nuth & Kääb 2011). In order to determine if there was an elevation bias in the DEM differences I binned all pixels of a given DEM difference into 200 uniform elevation classes covering the entire elevation range of the underlying reference DEM. I then calculated the median elevation difference for each elevation class before searching for the best fitting 1st, 2nd and 3rd order polynomial function to describe the relationship between the median elevation difference and the actual elevation (Figure 5.1a). For this step, I only considered elevation classes with more than 500 pixel values in order to omit classes containing only a small number of values, which are more likely to be influenced by outliers. I visually checked the three polynomial functions and selected the one that best fitted the median values. I then created a new raster with the same dimensions as the DEM difference. For each pixel of this new raster, I calculated the elevation dependent bias by using the best fitting polynomial function and the reference DEM as input data. By subtracting this new raster showing the spatial distribution of the elevation bias from the DEM difference, I obtained a DEM difference with minimised elevation bias.

In addition to performing an elevation dependent bias correction as suggested by Nuth and Kääb (2011), I also performed an aspect dependent bias correction. I did this in the same way as the elevation dependent bias correction except that I used an aspect map derived from the reference DEM instead of the reference DEM itself. I made this correction because there was a slight aspect dependent bias that was evident in some of the DEM differences. However, the effect of this correction was usually quite small, as the co-registration had already corrected for the horizontal shift of the DEMs, which is the main source of the aspect dependent bias (Figure 5.1b).

The elevation and aspect dependent bias correction was carried out for all DEM differences with the exception of the DEM difference DP-20/22. The reason for that is, that on 10 April 2020, when the first DEM of this DEM pair was acquired, the landscape was snow covered. If one were to determine the elevation dependent bias of the DEM difference DP-20/22 as explained in this section, one would mainly measure the elevation bias due to snow. This is because the elevation dependent bias due to snow is in the order of metres, whereas the bias due to errors in DEM generation is in the order of decimetres. The same applies to the aspect bias, where the greater snow depths on the northern slopes compared to the southern slopes would drown out the effective aspect bias. In order to be able to use the DEM

difference DP-20/22 to quantify volume changes despite the snow bias, I proceeded as follows. I searched for a reference area in the DEM difference DP-20/22 that is as similar as possible to the area of interest in terms of aspect, elevation and topography and for which no volume change is to be expected. I then determined the mean elevation change of the reference surface. Assuming that this elevation change is exclusively due to the snow cover and corresponds to that in the area of interest, I was able to determine the effective volume change in the area of interest.

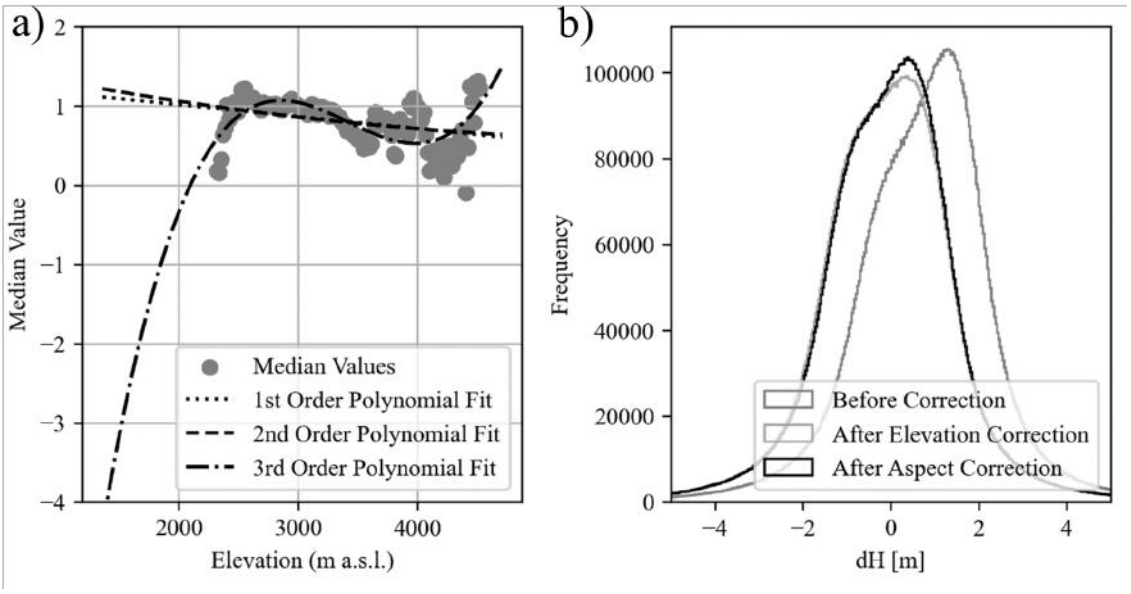

Figure 5.1: Graph **(a)** shows the elevation dependent bias for the DEM difference DP-19/23 with the three best fitting polynomial functions. Graph **(b)** shows the pixel distribution regarding the surface elevation difference before and after applying the elevation and the aspect dependent bias correction. It can be seen that the elevation-dependent bias correction has a significantly greater impact than the aspect-dependent bias correction.

5.1.3 Jitter Correction

The Pléiades satellite platform is known to have low-amplitude along-track undulating biases at a frequency of about 1 Hz (Deschamps-Berger et al. 2020). This non-systematic linear error is thought to be caused by unrecorded pitch variations of the satellite, commonly referred to as 'jitter' (Nuth & Kääb 2011). The resulting undulations have an amplitude in the order of a few decimeters to more than a meter and a wavelength of about 4km (Berthier et al. 2024; Deschamps-Berger et al. 2020). To correct for this error, I implemented an additional step in the DEM difference correction process for all DEM differences that were generated on the basis of at

least one Pléiades DEM (Figure 5.2).

To measure the amplitudes and wavelengths of the undulations, I calculated the median value for each row of the DEM difference, taking into account only those areas assumed to be stable. The reason for choosing the median rather than the mean value to determine the undulations properties, is its stability against outliers. Assuming that the row median values of stable terrain should theoretically equal to zero, the actual values are thought to primarily reflect the error induced by the jitter effect. This assumption is supported by the fact that the DEM differences show clear stripes in the cross-track direction that cannot be explained by natural processes in the landscape. By subtracting the median value from each pixel in the corresponding row, I obtained a corrected DEM difference.

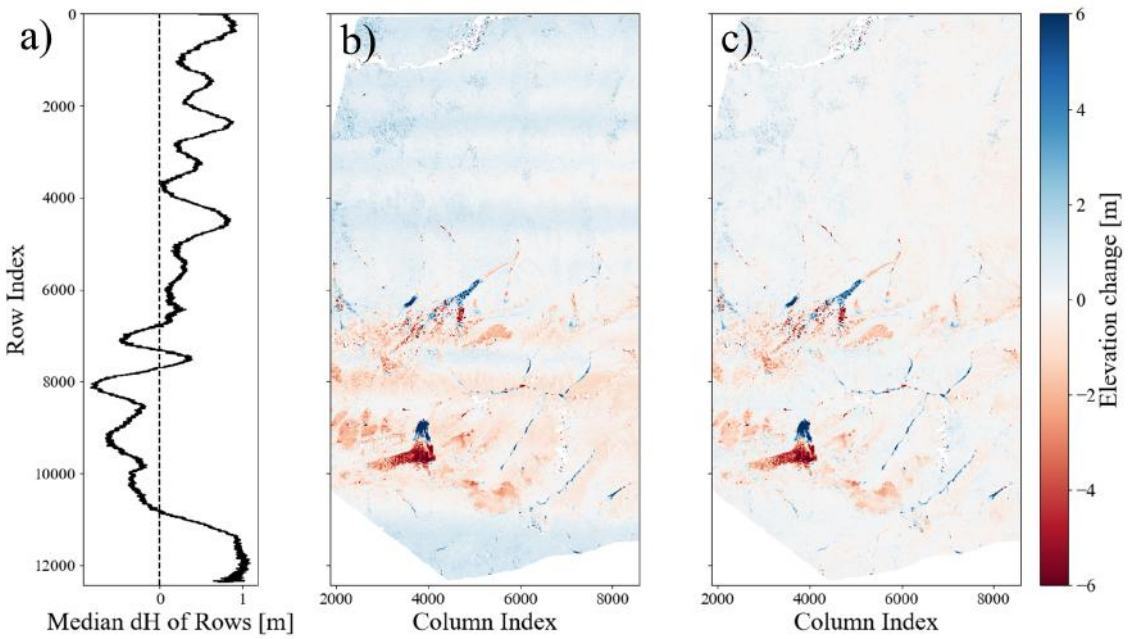

Figure 5.2: Visualisation of the jitter correction using the example of the DEM difference DP-22/23. Figure **(a)** shows the undulations of the mean surface elevation difference per row (only stable terrain considered), which are due to the jitter effect. **(b)** DEM difference before jitter correction with horizontal stripes. **(c)** DEM difference after jitter correction. **(b, c)** Pléiades.

5.2 DEM Difference Analysis

The analysis of the generated DEM differences is presented in this chapter. The first section describes how I estimated the uncertainty of the DEM differences. How I used the DEM differences to quantify volume changes in the landscape is described in the second section.

5.2.1 Uncertainty Estimation

I used a method proposed by Berthier et al. (2018) to estimate the uncertainty of the DEM differences. For this I used a freely available python code from Jacquemart (2019). The Berthier method is an empirical uncertainty estimation where the stable terrain of a DEM difference is iteratively tiled into n^2 tiles, with n ranging from 2 to 200. In each iteration, the median is calculated for each tile before the mean absolute error (MAE) is calculated over all tiles. The linear regression that best fits the relationship between the natural logarithm of the tile size and the MAE is then determined. The resulting function allows estimating the error in quantifying volumetric changes based on the size of the area affected. As expected, a significant decrease in MAE with increasing tile size was observed for all DEM differences (Figure 5.3a).
In addition to the correlation between the size of the analysed area and the MAE, I also investigated the relationship between the slope angle and the MAE by assigning all pixels within the stable terrain of a DEM difference to one of 30 slope classes according to their geographical location. I then calculated the MAE for each slope class. The analysis of the relationship between the slope angle and the MAE showed that the MAE is very constant in areas with slope angles up to 40°, but increases rapidly thereafter (Figure 5.3b). Increasing MAEs of DEM differences with increasing slope are probably related to the decreasing vertical accuracy of DEMs with increasing slope discussed in Section 4.1. As the areas of interest in this thesis are almost exclusively located in areas with a slope angle of less than 40°, this slope dependent increase in error does not affect the results of this thesis significantly.
As the DEM difference DP-18/19 covers a very small area and contains little stable terrain, it was not possible to apply the Berthier method to this DEM difference. To estimate the uncertainty of the DEM difference DP-18/19, I used the same equation as for the DEM difference DP-14/18, which has the largest uncertainty of all the DEM differences analysed that contain at least one of the DEMs of 2018 and 2019.

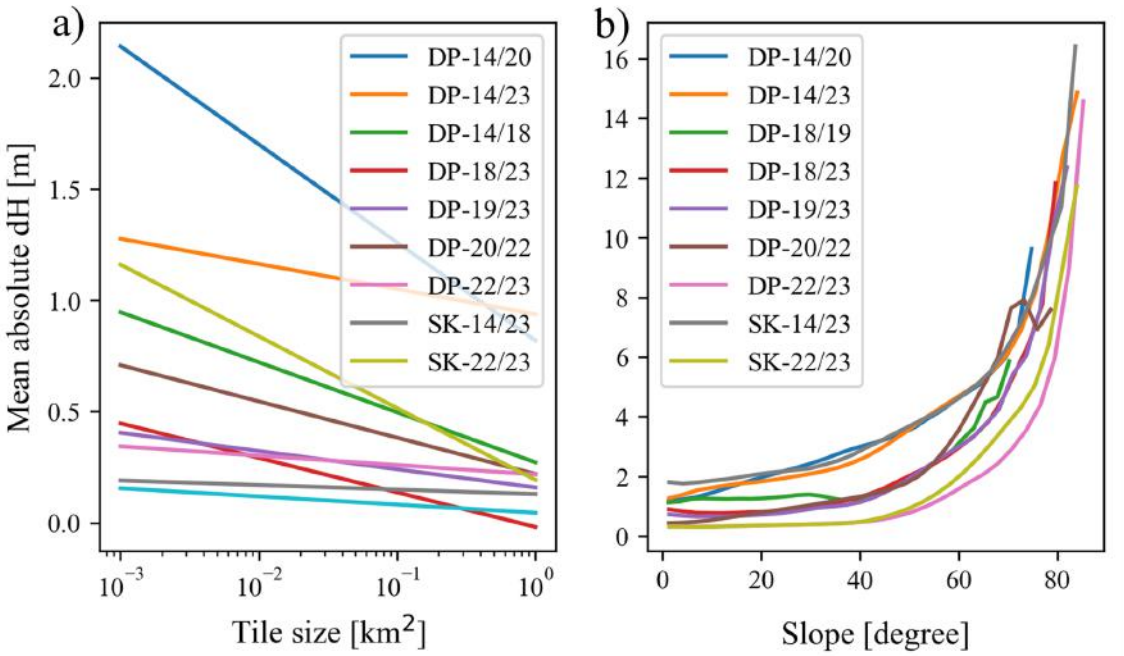

Figure 5.3: Graph **(a)** shows that with increasing tile size, the mean surface elevation difference decreases for all DEM differences. In other words, the relative uncertainty in the determination of volume changes is reduced the larger the area under analysis is. Graph **(b)** shows the relationship between the mean surface elevation difference of the DEM differences and the slope angle. It can be seen that the mean surface elevation difference increases sharply from a slope of 40°.

In addition to the general uncertainty estimate based on the method of Berthier et al. (2018), there are additional sources of uncertainty that need to be considered for some of the DEM differences. For example, the snow cover correction for the DEM difference DP-20/22 (cf. Section 5.1.2) is one source of uncertainty. To account for this, I have multiplied the average snow depth of the reference area by the area of interest and added this volume to the general uncertainty estimate. Another source of uncertainty arises when the areas analysed contain artefacts, as is the case in DEM difference DP-18/19. The exposed area is only very slightly covered by an artefact. Analysis of satellite imagery suggests that it is very likely that only a small volume reduction has occurred in this area. Some areas of interest on the surrounding slopes were slightly more covered by artefacts. As small changes in elevation are to be expected in these areas, I excluded pixels with elevation changes greater than 15 m and less than -15 m when quantifying volume changes. I then calculated the mean value of all pixels considered and multiplied it by the total area of interest. This step significantly reduces the error. Therefore, I did not adjust the uncertainty estimate for volume changes determined on the basis of the DEM

difference DP-18/19. Another potential source of uncertainty is regions in the DEM differences with no data. For DEM differences that have regions with no data values, I used the 'fill nodata' tool in QGIS before quantifying volume changes. Using this tool, I calculated the values for the no data regions from the surrounding pixel values within a 20 m radius based on inverse distance weighting (QGIS 2024). This allowed me to fill relatively small 'holes' in the DEM differences, while larger areas of no-data values were not interpolated using this method. These areas of no data were not included in the quantification of volume changes. As there is little overlap between these regions and the areas of interest, I did not expect any significant resulting uncertainties.

5.2.2 Quantification of Volume Changes

I analysed the DEM differences using QGIS, a free and open source geographic information system. To quantify the volume changes, I first created a polygon covering the area of interest. I then used the zonal statistics plugin with a DEM difference and at least one polygon as input data. The zonal statistics plugin allows the calculation of different statistics for each polygon, of which I needed the two statistics 'count' and 'mean'. The function 'count' represents the number of pixels within a given polygon and returns the area by multiplying it by the grid cell size of the DEM difference. The function 'mean' calculates the mean pixel value within a given polygon, i.e. the mean surface elevation change. By multiplying the area by the mean value, I was able to get the total change in volume within a given polygon. To convert volume changes to mass changes for the determination of glacier mass balances, I used an estimated glacier average density of 850 $kg \cdot m^{-3}$ with an uncertainty range of $\pm$ 60 $kg \cdot m^{-3}$ as suggested by Huss (2013).

5.3 Climate Analysis

The analysis of climatic changes and the comparison of the period 2014-2023 with long-term averages in the high mountain areas of central Tajikistan is based on a dataset of various meteorological variables for the period between 1 January 1970 and 30 September 2023. For the analysis I used the two variables temperature and precipitation.

To assess current climate conditions and the climate change in the high mountain areas of central Tajikistan, I worked with climatalogical standard normals, also known as climate normals. Climate normals are defined by the World Meteorolog-

ical Organisation (WMO 2017a) as averages of climatological data calculated for consecutive 30-year periods (e.g. 1 January 1981-31 December 2010). Climate normals have two main functions: They provide an implicit prediction of the conditions most likely to occur in the near future, and they serve as a stable benchmark against which long-term changes in climate observations can be compared (WMO 2017b). The 1961-1990 climate normal has been defined as the standard reference period for long-term assessments of climate change (WMO, 2017 No. 1203). As the dataset used for the climate analyses in this thesis only includes data from 1970 onwards, I have instead used the 1971-2000 climate normal to assess climate change. As a consequence, the observed climate change cannot be compared with values from other regions where the 1961-1990 climate normal has been used. Nevertheless, this approach makes it possible to study long-term climate trends. In addition to the climate normal 1971-2000, I also analysed the two climate normals 1981-2010 and 1991-2020. The comparison of these two climate normals with the 1971-2000 climate normal makes it possible to assess the long-term climate changes.
The 1991-2020 climate normal is the most recent climate normal and therefore best describes the climate that can currently be expected in the high mountain areas of central Tajikistan. I compared the mean annual temperature and mean annual precipitation of the years 2014-2022, which are the focus of this thesis, with the climate normal of 1971-2000. This made it possible to judge whether the last few years have been above or below average in terms of temperature and precipitation. It was not possible to carry out this analysis for 2023 because meteorological data is only available until the end of September 2023.
In addition to the climate normals, which show the long-term climate trends, I have calculated the 9-year moving average for the mean annual temperature and the mean annual precipitation. The 9-year moving average illustrates the ongoing medium-term climate changes particularly well.

5.4 Analysis Approach

This section describes the conceptual structure of my analysis and explains certain decisions in the way of proceeding, mostly related to data availability.
I used two different approaches to analyse the landscape impacts of glacier detachments in the Degilmoni Poyon and Shuraki Kapali catchments. In the Degilmoni Poyon catchment I focused on the 'exposed area', the 'surrounding slopes' and the 'runout zone' and quantified the observed volume changes in these areas. In the

Shuraki Kapali catchment I focused on the 'glaciated areas' and the 'runout zone', and mainly used a qualitative approach to describe how these changed. The reason for the different approaches is the availability of DEMs and the frequency of mass movements in the two catchments. For the Degilmoni Poyon catchment, a DEM is available for every year between 2018 and 2023, with the exception of 2021. Furthermore, the glacier detachment in 2019 is the only major mass movement that has occurred in the Degilmoni Poyon catchment in recent years. Both the short time steps between the DEMs and the manageable number of ongoing processes make it easier to reconstruct the evolution of the different areas. Volume changes can thus be quantified and assigned to a particular process. This is not possible for the Shuraki Kapali catchment, where only three DEMs are available (2014, 2022, 2023) and several spatially overlapping mass movements occurred between 2014 and 2023. The volume changes observed in the DEM difference Sk-14/22 are therefore difficult to attribute to a specific process. This has led me to use mainly satellite imagery for the analysis of the Shuraki Kapali catchment, which has the advantage of a much higher temporal resolution. However, this also means that only qualitative statements can be made about the volume changes observed.

Another difference in the analysis of the two catchments concerns their runout zones. In the Degilmoni Poyon catchment, I analysed the spatial distribution of deposits from the 2019 event and how the volume of these deposits changed over time. In the runout zone of the Shuraki Kapali catchment, this was again not feasible due to the lower temporal resolution of the DEMs. However, in the runout zone of the Shuraki Kapali catchment, it was possible to analyse the impact of glacier detachments on inhabited areas using satellite imagery. In the Degilmoni Poyon catchment this would not be possible as there has not been an documented event with such far-reaching consequences.

In order to contextualise the observed developments in the Degilmoni Poyon and Shuraki Kapali catchments, I investigated the climatic conditions in the high mountain regions of central Tajikistan and the current state of the glaciers in the Petra Pervogo range. For the latter I analysed the mass balance of seven glaciers between 9 September 2018 and 4 September 2022 (Figure 5.4). The reason why I chose this period is based on a compromise between choosing the longest possible study period and obtaining the most accurate results. The DEMs of 2018 and 2022 both have a good vertical resolution of 2 m (which is not the case for the DEM of 2014). In addition, in both September 2018 and September 2022 even the highest peaks of the Petra Pervogo range were almost free of snow (which was not the case in 2023).

The overlap between the 2018 and 2022 DEMs is quite small and therefore does not cover many glaciers. The seven glaciers I examined in more detail are the only ones that lie entirely within this overlap and are not covered by a cloud or influenced by some other artefact.

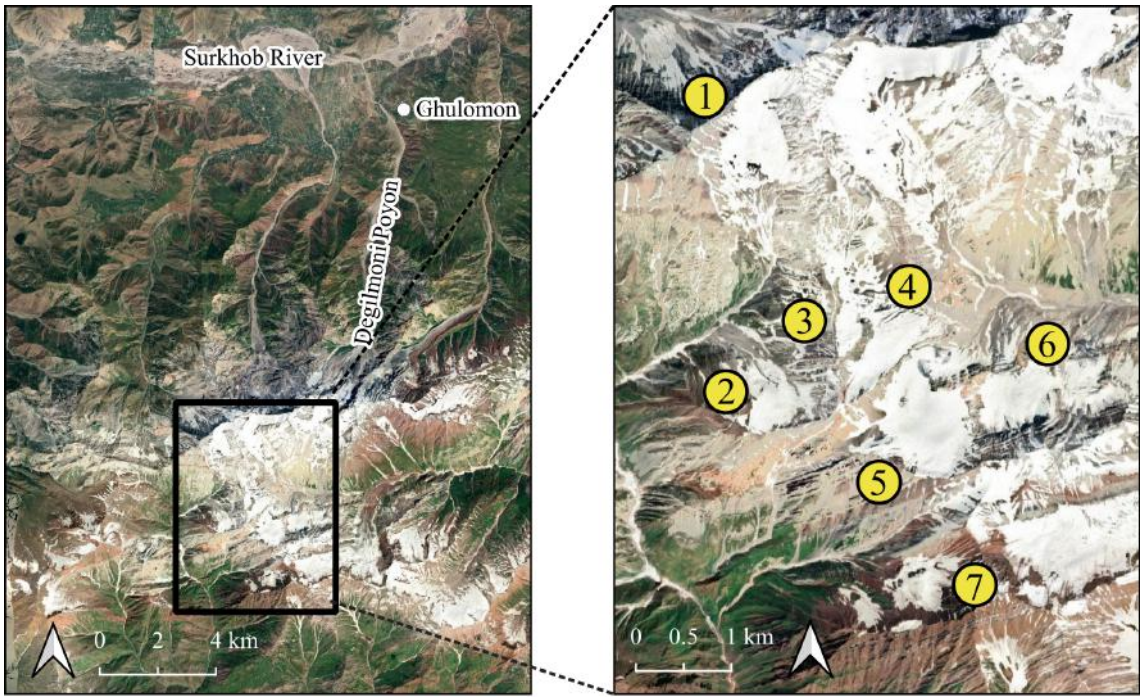

Figure 5.4: Location of the seven glaciers whose mass balance was analysed for the period 2018-2022. The numbers in the right image are to identify the glaciers clearly and are used in Table 6.3. Google, Maxar Technologies.

6. Results

6.1 Regional Context

The following two sections present the results of the analyses of the current state of climate and glaciers in the Petra Pervogo Range. These results serve to place the findings of the detailed analyses of the Degilmoni Poyon and Shuraki Kapali catchments in a broader context. The climate analysis is limited to the two variables of temperature and precipitation and is based on a downscaled and bias-corrected dataset for a meteorological station located in the Jiragol district at 3369 m. The analysis of the current state of the glaciers in the Petra Pervogo Range comprises the study of 124 glaciers for the period 2019-2023. For a more complete picture, the results are combined in the section 6.1.2 with those of Leinss et al. (2021), who performed similar analyses for the period 1973-2019.

6.1.1 Climate

Temperature

Temperatures in the high mountain areas of central Tajikistan have risen significantly since 1970. This is reflected in the climate normals, which increased from -1.89 °C to -1.74 °C to -1.51 °C for the periods 1971-2000, 1981-2010 and 1991-2020. This corresponds to a long-term temperature increase of 0.38 °C. The clear temperature increase can also be seen in Figure 6.1, which shows the annual temperature deviation from the 1971-2000 climate normal and the 9-year moving average deviation. Since the turn of the millennium, only three years (2000, 2005 and 2012) have been cooler than the 1971-2000 climate normal. All were less than 0.5 °C cooler than the long-term average. Over the same period, 13 years were more than 0.5 °C warmer than the long-term average, with three of them exceeding 1 °C (2001, 2016 and 2022). These three years are also the years with the highest annual mean temperature since the beginning of the data series in the year 1970. The accumulation

of above-average warm years since the turn of the millennium is also reflected in the 9-year moving average. It fluctuated around 0 °C between 1970 and 2000, before rising by more than 0.6 °C in 18 years between 2000 and 2018.

Table 6.1 compares the mean annual temperatures for the period 2014-2022, during which the glacier detachments investigated in this study took place, with the climate normals 1971-2000, 1981-2010 and 1991-2020. It is striking that the last few years have not only been warmer than the 1971-2000 climate normal. Compared to the current climate normal 1991-2020, all annual mean temperatures are also above average, with the exception of 2014, which was 0.23 °C cooler.

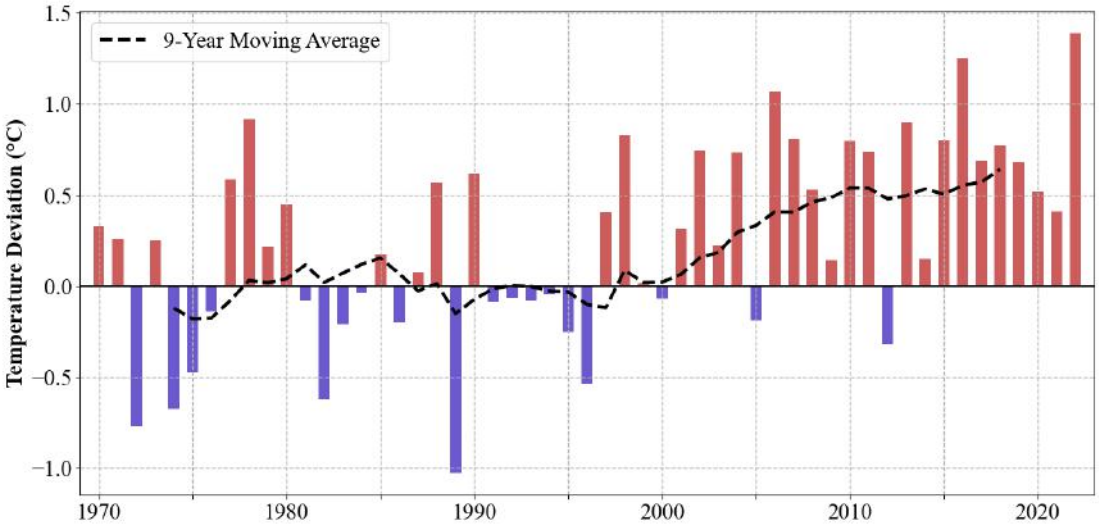

Figure 6.1: Long-term trend of mean annual temperatures in high mountain areas of central Tajikistan since 1970, as a deviation from the 1971-2000 climate normal. Blue bars indicate years that were cooler and red bars warmer than the norm. The dashed line shows the 9-year moving average.

Precipitation

Unlike temperature, precipitation in the high mountain areas of central Tajikistan shows no clear trend over the last 50 years. For the 1971-2000 climate normal, the average annual precipitation was 1250 mm, for 1981-2010 1314 mm and for 1991-2020 1206 mm. Figure 6.2 shows a clustering of drier and wetter years compared to the 1971-2000 climate normal at the beginning of the data series. From 1970 to 1985, all but one year were drier than average, followed by eight wetter than average years. Since 1986, dry and wet years have alternated more regularly. However, the last six years of the data series have all been drier than average and include the three

Table 6.1: Mean annual temperature in high mountain areas of central Tajikistan compared to the climate normals 1971-2000, 1981-2010 and 1991-2020.

		Deviation from Climate Normals [°C]		
Year	**Mean Temp. [°C]**	1971-2000	1981-2010	1991-2020
2014	-1.74	0.15	0.00	-0.23
2015	-1.09	0.80	0.65	0.42
2016	-0.64	1.25	1.10	0.87
2017	-1.20	0.69	0.54	0.31
2018	-1.12	0.77	0.62	0.39
2019	-1.21	0.68	0.53	0.30
2020	-1.37	0.52	0.37	0.14
2021	-1.48	0.41	0.26	0.03
2022	-0.51	1.39	1.24	1.01

driest years of the whole data series (2019, 2020, 2021).These developments are also reflected in the 9-year moving average, which shows a partly strongly positive trend from the 1980s to the mid-1990s and a subsequent decline until the 2010s. Towards the end of the 2010s, the 9-year moving average returned to a level similar to that of the 1970s.

A comparison of the years 2014-2022 with the climate normals 1971-2000, 1981-2010 and 1991-2020 shows an uneven distribution of wetter and drier years (Table 6.2). The years 2014-2016 had average to slightly above-average precipitation, depending on which climate normals are used for comparison. Between 2017 and 2022, all years were drier than average. This period also includes the three driest years of the entire measurement series (2019, 2020 and 2021), which brought between 35 % and 42 % less precipitation than would be expected according to the current climate normal 1991-2020.

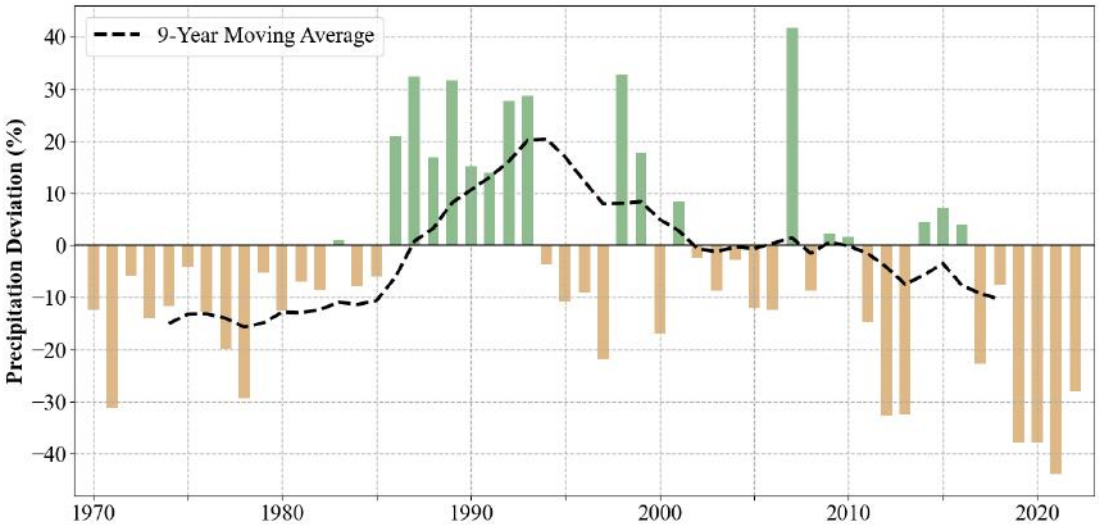

Figure 6.2: Long-term trend of average annual precipitation in high mountain areas of central Tajikistan since 1970, as deviation from the climate normal 1971-2000. Brown bars indicate years that were drier and green bars wetter than normal. The dashed line shows the 9-year moving average.

Table 6.2: Mean annual precipitation in high mountain areas of central Tajikistan compared to the climate normals 1971-2000, 1981-2010 and 1991-2020.

		Deviation from Climate Normals [%]		
Year	**Precipitation [mm]**	1971-2000	1981-2010	1991-2020
2014	1303	4.3	-0.8	8.0
2015	1339	7.1	1.9	11.0
2016	1302	4.2	-0.9	7.9
2017	965	-22.8	-26.6	-20.0
2018	1155	-7.6	-12.1	-4.2
2019	776	-37.9	-40.9	-35.6
2020	778	-37.8	-40.8	-35.5
2021	701	-43.9	-46.6	-41.9
2022	899	-28.1	-31.6	-25.5

6.1.2 Glaciers

Surging Glaciers

Of the 124 glaciers studied, five have either been surging in recent years or are still in a surging phase. Three of these five glaciers showed the typical behaviour of surge-type glaciers, with either an increase in elevation at the terminus and a decrease further up (active phase), or a volume loss at the terminus and a mass gain

in the upper parts (quiescent phase). This characteristic behaviour was much less pronounced on two other glaciers. In both cases, rockfall events preceded the surges, suggesting that they are not surge-type glaciers in the classical sense. The surges were probably triggered by the mass loading caused by the rockfall. Coordinates indicating the location of the glacier surges and further information, including the findings of Leinss et al. (2021), are provided here:

- 38.937°N, 70.695°E: the first documented surge started in 1993 and ended in 1996 (Leinss et al. 2021). After a quiescent phase, the glacier started surging again in 2019 and was still surging in 2023. During the second surge, the glacier advanced by about 100 m in the period 2019-2023 and, based on the DEM difference DP-18/23, the thickness of the glacier tongue increased by more than 50 m in some places.

- 38.994°N, 70.725°E: the glacier began to surge in June 1995, advancing 2.3 km within seven months (Leinss et al. 2021). After retreating, a second surge phase occurred between June 2015 and July 2016, during which the glacier advanced 5 km (Leinss et al. 2021).

- 38.992°N, 70.830°E: the glacier surged in autumn 1993 and again in 2010/2011, both times entering the valley of the Shuraki Kapali catchment (Leinss et al. 2021). In 2023, the glacier was still in a quiescent phase.

- 39.024°N, 70.866°E: between 2016 and 2019, the glacier has been surging. Deposits of a rockfall that occurred between 23 June 2016 and 25 July 2016 are clearly visible on the glacier (Figure A.1). It is possible that there is a link between the rockfall event and the advance of the glacier of about 50 m (Figure A.2).

- 39.021°N, 70.899°E: the glacier is surging since at least August 2016. The lack of high-resolution satellite imagery prevents a more precise statement. Two major rockfall events have been identified, one between 28 May 2012 and 29 June 2012 and the other between 23 July 2022 and 06 August 2022, resulting in widespread deposits on the glacier (Figure A.1). The increase in the thickness of the glacier tongue and an advance of about 40 metres could possibly be attributed to these rockfall events (Figure A.2).

Glacier Detachments

None of the 124 glaciers analysed experienced glacier detachment in the period 2019-2023, except for the glacier in the Degilmoni Poyon catchment. Leinss et al. (2021) also found no glacier detachments outside the Degilmoni Poyon and Shuraki Kapali catchments for the period 1973-2019.

State of 'Normal' Glaciers

The seven glaciers analysed, all of which have experienced neither a detachment nor a surge in recent years, have negative changes in surface elevation for the period between 09 September 2018 and 04 September 2022 (Table 6.3). The mean values range from -2.51 ± 0.10 m to -3.77 ± 0.12 m, corresponding to melt rates of -0.63 ± 0.03 ma^{-1} to -0.94 ± 0.04 ma^{-1}. This range shows that, although all of the glaciers analysed have experienced a loss of volume in the period 2018-2022, there are significant differences in the magnitude of the loss. This is not surprising, as they also differ in terms of location characteristics. Glacier no.1, with a melt rate of -0.63 ± 0.03 ma^{-1}, is located at a mean elevation of 4160 m on a south facing slope. The glaciers nos.2-6 have mean elevations between 3750 and 4000 m and face north to northeast. Their melt rates range from -0.79 ± 0.03 ma^{-1} to -0.94 ± 0.04 m/a. Glacier no. 7 is located lower than most of the other glaciers at 3770 m in a west-facing valley and has a melt rate of -0.64 ± 0.03 ma^{-1}. It is noticeable that glacier no.1 (-0.63 ± 0.03 ma^{-1}) and glacier no.7 (-0.64 ± 0.03 ma^{-1}) have significantly lower melt rates than the other glaciers studied. The fact that glacier no.1 has a comparatively low melt rate is not entirely surprising given its elevation. However, the big difference to the melt rates of the glaciers nos.2-6 is surprising because of the southern exposure of glacier no.1. The low melt rate of glacier no.7 is even more surprising given its low elevation. It is evident that the two variables elevation and aspect are not sufficient to explain the different melt rates of the studied glaciers. Other factors must also play an important role. What distinguishes the two glaciers with the lowest melt rates, no.1 and no.7, from the others is the fact that they are surrounded by steep slopes. This is an indication that the contribution of avalanches and/or the shielding effect have a decisive influence on the melt rate.

Apart from the seven glaciers described above, I have not systematically analysed the melt rates of the glaciers in the Petra Pervogo range. However, most of the other glaciers also appear to be retreating during this period. Excluding glaciers that experienced a detachment or are surging, the DEM differences DP-14/23 and SK-14/23 show an average negative change in elevation for all glaciers.

Table 6.3: Mass balances of seven glaciers in the Petra Pervogo range between 09.09.2018 and 04.09.2022.

Glacier	no.1	no.2	no.3	no.4	no.5	no.6	no.7
Area [ha]	8.14	4.80	3.04	7.78	22.66	14.80	5.43
Aspect	S	N	NE	NE	N	N	W
Slope [°]	18.7	23.2	23.1	16.3	15.2	15.8	20.3
Lowest point [m]	4040	3680	3860	3780	3680	3570	3670
Highest point [m]	4350	3950	4130	4070	4170	3920	3880
Mean elevation [m]	4160	3830	3960	3910	3920	3760	3770
Mean dH [m]	-2.51	-3.39	-3.77	-3.36	-3.17	-3.29	-2.57
	±0.09	±0.08	±0.07	±0.08	±0.10	±0.09	±0.08
Melt rate [m/a]	-0.63	-0.85	-0.94	-0.84	-0.79	-0.82	-0.64
	±0.02	±0.02	±0.02	±0.02	±0.02	±0.02	±0.02
Mass balance	-0.54	-0.72	-0.80	-0.71	-0.67	-0.70	-0.54
[m w.e.yr^{-1}]	±0.06	±0.07	±0.08	±0.07	±0.07	±0.07	±0.06

6.2 Degilmoni Poyon Catchment

The following three sections show how the areas of the Degilmoni Poyon catchment affected by the glacier detachment in 2019 have developed by 2023. The first section describes developments within the exposed area. The second section focuses on the surrounding slopes of the exposed area and the extent to which volume changes there are related to the glacier detachment. The deposition of the detachment in the runout zone and its evolution over time are described in the third section.

6.2.1 Exposed Area

The area exposed by the glacier detachment in the Digilmoni Poyon catchment on 03 August 2019 is about 0.25 km^2 and extends from 2800 m to 3350 m. Based on the DEM difference DP-18/19, the detached volume is $8.72 \pm 0.39 \times 10^6$ m^3, which corresponds to an average erosion depth of 35 m, reaching values up to 92 m (Figure 6.3). During the following four years, between September 2019 and September 2023, new material with a total volume of $3.07 \pm 0.08 \times 10^6$ m^3 (3.1 ma^{-1}) was deposited on the previously exposed area. This means that by autumn 2023, one third of the volume loss caused by the glacier detachment on 3 August 2019 had been compensated. A closer look at the temporal course of the volume increase reveals strong fluctuations. An increase of $0.81 \pm 0.56 \times 10^6$ m^3 (1.4ma^{-1}) was observed between 10 April 2020 and 3 September 2022, and a further $0.66 \pm 0.04 \times 10^6$ m^3 (2.7 ma^{-1}) until 4 September 2023. The remaining $1.61 \pm 0.68 \times 10^6$ m^3 (9.4 ma^{-1}) must therefore have accumulated on the exposed surface between the event on 3 August

2019 and 10 April 2020, hence within half a year.

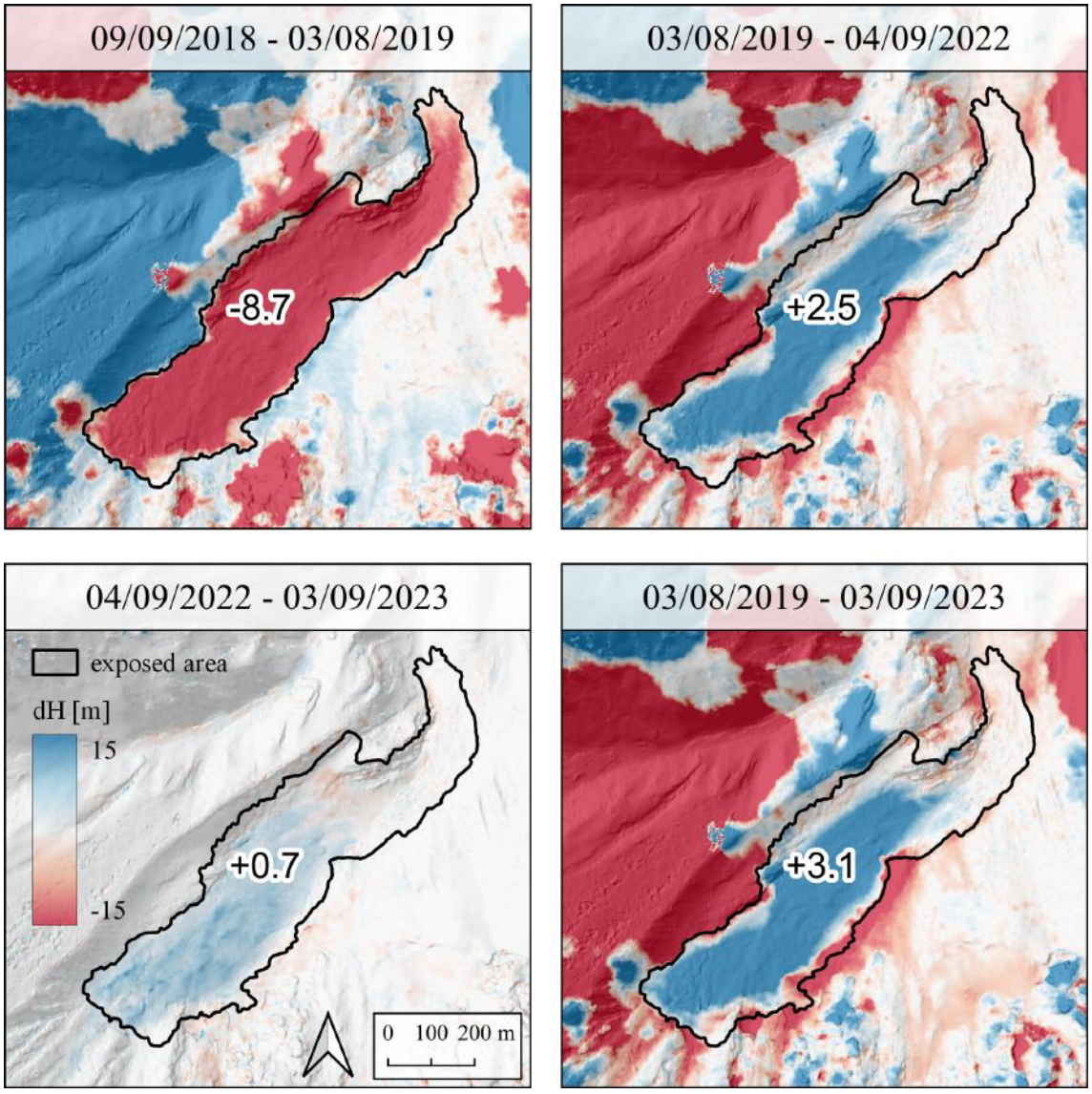

Figure 6.3: Surface elevation changes in the area exposed by the detachment in 2019 over four different time periods. The numbers show the volume change in millions of cubic metres within the exposed area. WorldView, Pléiades.

6.2.2 Surrounding Slopes

There are two possible causes to explain the mass accumulation observed on the area exposed by the glacier detachment and described in section 6.2.1: regeneration of the glacier ice or redistribution of snow, ice and lithic material on the exposed area, or a combination of both. In order to identify the driving processes behind the mass accumulation, I studied the slopes above the exposed area. Taking into account the

DEM difference DP-19/23, I identified six areas adjacent to the exposed area that had a clearly negative height difference between 3 August 2019 and 3 September 2023 (Figure 6.4). These six areas are discussed in detail in the following list:

Area I) A channel filled with snow and ice leads from the southwest to the exposed area. From 3 August 2019 to 3 September 2023, this channel recorded a volume loss of $-0.36 \pm 0.03 \times 10^6$ m^3. The entire loss is attributable to the period from 10 April 2020 to 4 September 2022 (DP-20/22). From 4 September 2022 to 3 September 2023, the volume in the channel even increased slightly again (DP-22/23). Satellite images from 25 August 2019 and 29 September 2024 also show that a comparable channel only about 500 m to the west of the investigated channel shows hardly any changes. The temporally limited volume loss and the comparison with the nearby channel indicate that the volume loss in the investigated channel was a reaction to the glacier detachment and cannot be explained by normal melting processes, at least for the most part. It can therefore be assumed that a large part of the lost volume of $-0.36 \pm 0.03 \times 10^6$ m^3 was mobilised and probably deposited on the exposed area.

Area II) The second area is also a channel filled with snow and ice that runs parallel to Area I. In the period from 2019 to 2023, this channel behaved practically the same as the one described under Area I and shows a volume loss of $-0.21 \pm 0.04 \times 10^6$ m^3. However, the changes in the channel are largely confined to its lower half. Again, it can be assumed that the snow and ice was mobilised from the channel as a result of the detachment and deposited on the exposed area.

Area III) A glacier in the south of the exposed area shows a large volume change of $-1.99 \pm 0.12 \times 10^6$ m^3. Its glacier tongue was connected to the glacier further down over a width of about 100 metres before the latter's detachment. Comparing the melt rate of this glacier with that of a nearby glacier for the period from 10 April 2020 to 3 September 2023, it is striking that they are almost identical (Figure A.3). This comparison is not possible for the period from 2019 to 2020 because the nearby glacier is covered by clouds in the DEM of 3 August 2019. Nevertheless, based on the comparison with the nearby glacier, it can be assumed that the observed volume loss of $-1.99 \pm 0.12 \times 10^6$ m^3 is due to normal climate related melting processes. This hypothesis is also supported by the results described in chapter 6.1.2, which show a significant decrease in

glacier volume for several glaciers in the Petra Pervogo range between 2018 and 2022.

Area IV) On the orographic right of the exposed area, there were remnants of the glacier that were not mobilised by the detachment in 2019. These are no longer visible in the satellite image of 4 September 2022. The DEM difference DP-19/20 shows that a large part of it had already collapsed in the first months after the detachment by 10 April 2020 and was most likely deposited on the exposed area. In total, Area IV experienced a volume loss of $-0.47 \pm 0.02 \times 10^6$ m^3.

Area V) Another channel approaches the centre of the exposed area from the south. This channel is also partially filled with snow and ice. While the two DEM differences DP-19/20 and DP-22/23 show no significant volume changes in the area of the channel, a clear volume loss can be seen in DEM difference DP-20/22. In addition, this DEM difference shows a deposition fan in the area where the channel joins the exposed area. In contrast to the two channels described above (Area I and Area II), the satellite images show that larger amounts of lithic material were also involved in the processes causing the volume loss. Overall, the channel experienced a volume loss of $-0.34 \pm 0.03 \times 10^6$ m^3 between 3 August 2019 and 3 September 2023.

Area VI) Above the lower part of the detached glacier, there is a glacial feature resembling a debris-covered glacier. Whether it is really a debris-covered glacier cannot be determined conclusively from the satellite images, but ice is visible in some areas. The DEM difference DP-19/23 shows that there is a decrease in height in the upper part of this glacial feature and a slight increase in height in the lower part. This indicates that the glacier feature is moving downwards, possibly due to the lack of back pressure caused by the glacial detachment. The sidewall formed by the former glacier between the glacial feature and the exposed area gradually collapsed between 2019 and 2023 and formed a debris cone that extends onto the exposed area. The whole area shows a volume loss of $-0.20 \pm 0.03 \times 10^6$ m^3 between 3 August 2019 and 3 September 2023.

In conclusion, it can be said that the volume lost in the different areas of the surrounding slopes, with the exception of Area III, was probably mostly deposited on the exposed area. Thus, in the Deglimoni Poyon catchment, a redistribution of mass has taken place between the surrounding slopes and the exposed area. Adding up the volume losses of these areas (excluding Area III), the volume deposited on the

exposed area between 3 August 2019 and 3 September 2023 is $1.56 \pm 0.15 \times 10^6$ m^3. However, it must be assumed that some of the redistributed snow and ice has already left the exposed area in the form of water by September 2023 due to climate-induced melting or melting during relocation processes. Unfortunately, it is not possible to determine this amount on the basis of the available data. However, even if all the redistributed material had still been on the exposed surface in September 2023, this would be $1.51 \pm 0.22 \times 10^6$ m^3 less than the observed volume increase on the exposed surface in the period from 3 August 2019 to 3 September 2023 (cf. chapter 6.2.1). Thus, about half of the volume increase on the exposed surface (or even more) cannot be explained by mass redistribution. As the exposed area extends from 2800 m to 3350 m, glacier growth is not expected under normal circumstances (cf. section 6.1.2). One likely explanation is that avalanche deposits are responsible for the fact that the volume nevertheless increased by $1.51 \pm 0.22 \times 10^6$ m^3. This seems also plausible looking at the DEM difference DP-22/23, where none of the six areas shows a significant loss of volume but the exposed area still experienced a volume increase of $0.66 \pm 0.04 \times 10^6$ m^3. This increase seems to be the result of avalanche deposits.

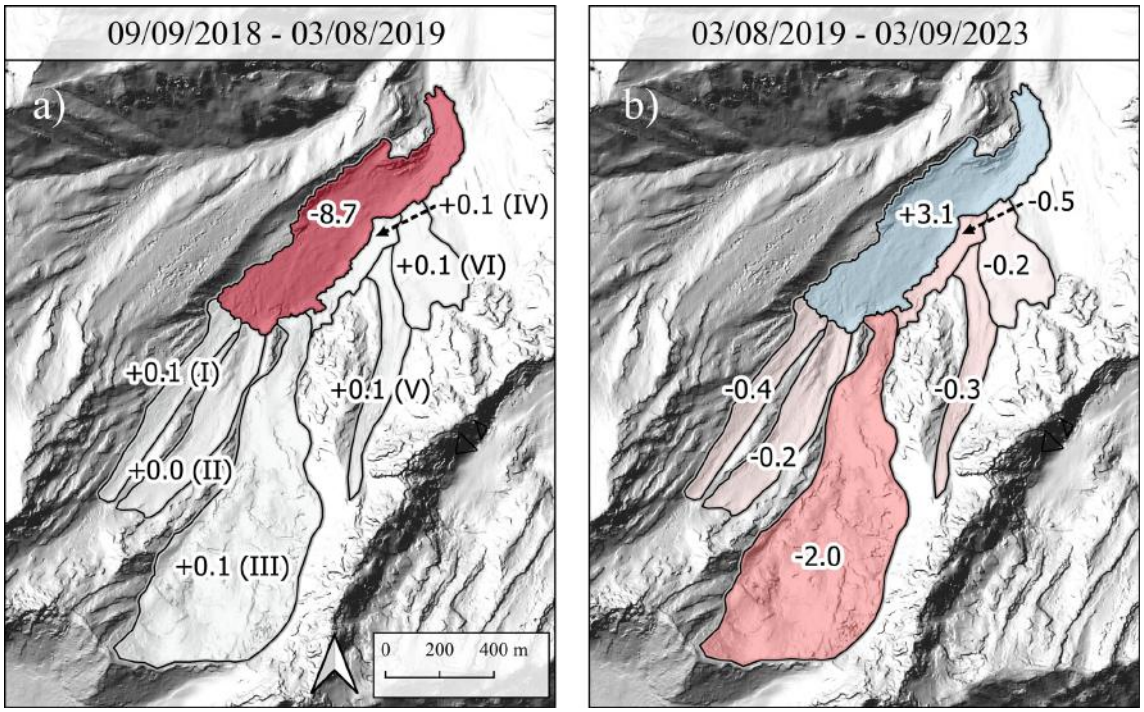

Figure 6.4: Volume changes in the exposed area and in six areas of the surrounding slopes. The Arabic numbers show the volume change in millions of cubic metres. **(a)** Volume changes before the detachment. The Roman numerals are used to number the surfaces (see section 6.2.2). **(b)** Volume changes after the detachment. **(a)** WorldView, **(b)** Pléiades.

6.2.3 Runout Zone

The detached mass of the 2019 event travelled 5.5 km downstream before stopping. The deposits are clearly visible in the DEM difference DP-14/20 (6.5). A volume increase of $7.57 \pm 2.20 \times 10^6$ m^3 was measured over the entire runout zone. Comparing this value with the volume of the detached glacier of $8.72 \pm 0.87 \times 10^6$ m^3, no significant difference can be identified. Nevertheless, it makes sense that the deposited volume tends to be lower than the detached volume. This is because it can be assumed that some of the ice melted and fine lithic material was washed out during the event itself and also afterwards up to 10 April 2020. Between 10 April 2020 and 4 September 2022, a volume loss of $7.13 \pm 0.50 \times 10^6$ m^3 was recorded in the runout zone, which is almost equivalent to the volume deposited by April 2020. No significant volume changes are observed between 4 September 2022 and 3 September 2023 ($0.10 \pm 0.30 \times 10^6$ m^3), probably because all the deposited ice had already melted by September 2022. The difference in volume between deposited and melted ice and washed out sediment, although not significant, may be explained by lithic material mobilised by the detachment and deposited in the runout zone.

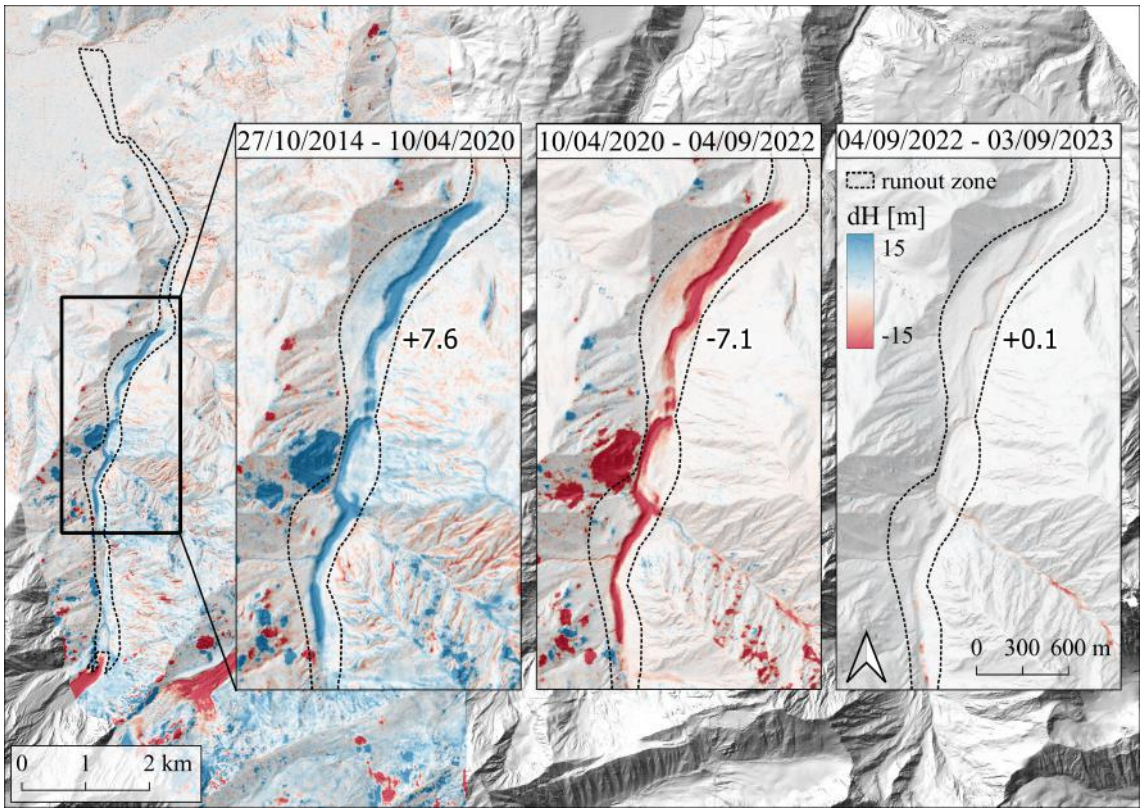

Figure 6.5: Evolution of detachment deposition in the runout zone over time, shown using three DEM differences. The numbers show the volume change in millions of cubic metres. TanDEM-X, WorldView and Pléiades.

Although ice deposits from the 2019 detachment melted within three years, traces of the detachment remain in the form of partially altered river courses. Figure 6.6 shows a particularly striking example of this in a river section about 3.5 km below the glacier. The course of the Degilmoni Poyon river has changed over a length of about 650 m in this section and is now up to 50 m to the west of its old course. The effect of this on the landscape can be seen in figure 6.6d. Along the new course of the river, the DEM difference DP-14/23 shows a clear decrease in height due to erosion. On average this decrease is 6.1 $\pm$0.7 m in the investigated area, but reaches values of up to 13.3 m in the cut bank of the first right curve.

Looking at the runout zone after the detachment in 2019, a vegetation-free trail of devastation can be seen stretching down the valley (Figure 6.7). By 2024, the vegetation had already recovered considerably. Although there are still some patches of missing vegetation, the appearance of the runout zone is very similar to that of 2008. Comparing the satellite images from 2008 and 2024, it is noticeable that there was hardly any vegetation in the area of the ice deposits even before the detachment. This was already noted by Leinss et al. (2021) and could indicate an earlier detachment. Closer inspection of the 2024 satellite image also reveals parallel striations in the upper part of the runout zone.

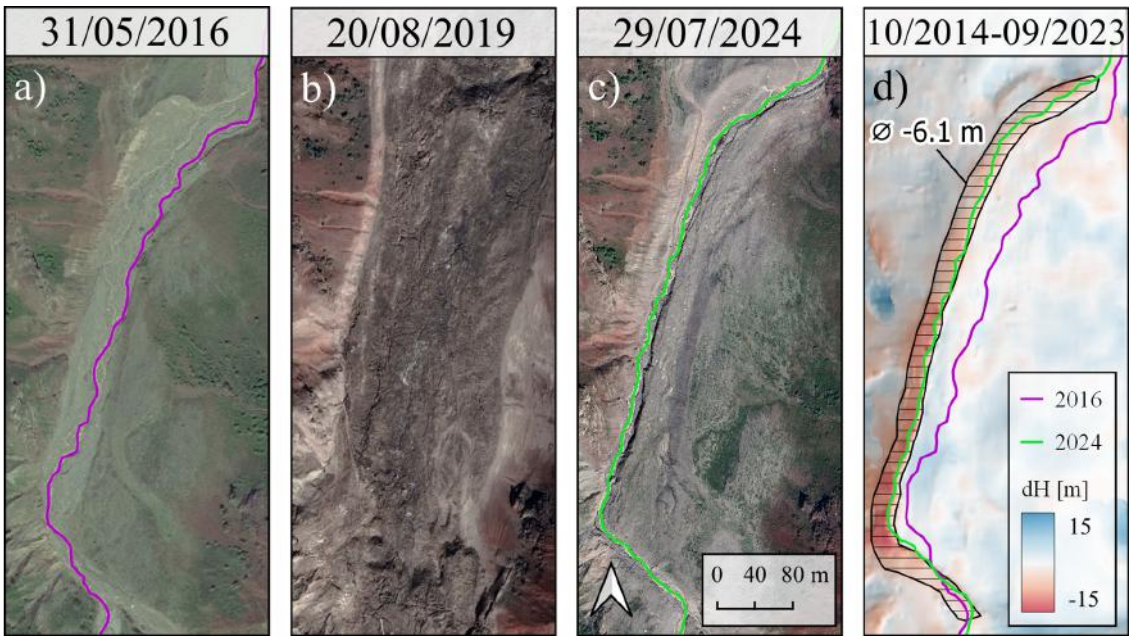

Figure 6.6: Development of a river section of the Degilmoni Poyon river under the influence of the detachment. **(a)** River course before the detachment (pink line). **(b)** The river section completely covered by the deposits of the detachment. **(c)** River course after the melting of the ice deposits (green line). **(d)** Comparison of the river course before and after detachment. The average surface elevation change in the striped area is 6.1 m. **(a-c)** © Google, Maxar Technologies; **(d)** TanDEM-X; Pléiades.

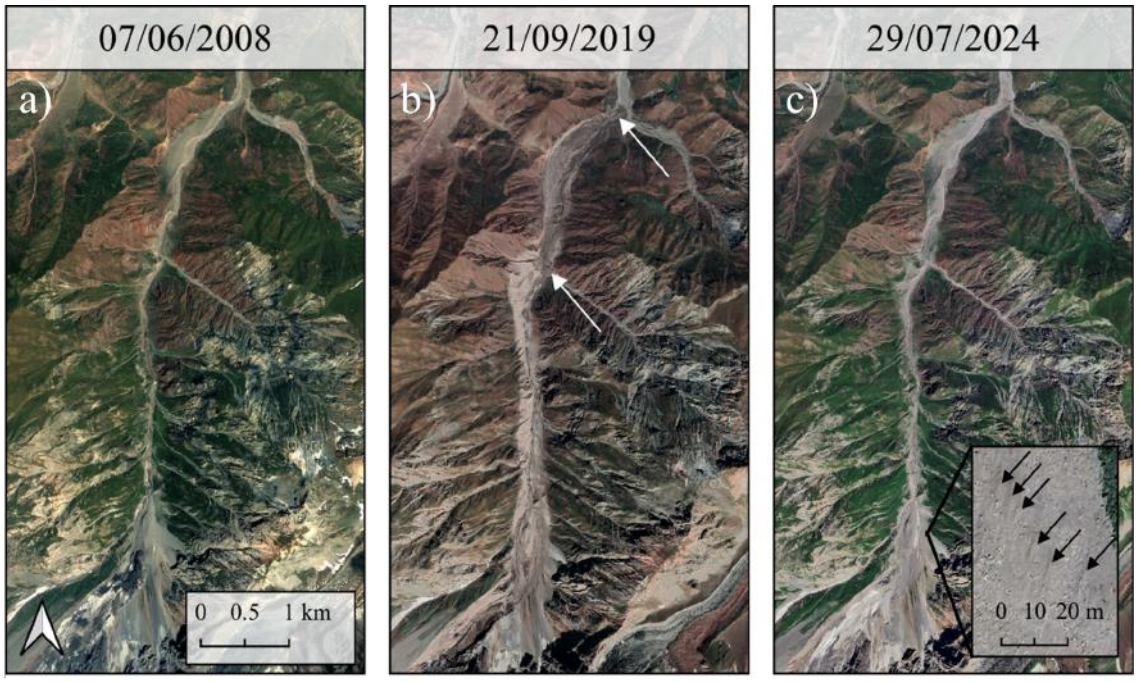

Figure 6.7: Comparison of the appearance of the runout zone in the Degilmoni Poyon catchment before the detachment **(a)**, barely two months after the detachment **(b)** and five years later **(c)**. The arrows in the image **(b)** show the beginning and end of the area where most of the deposits are located. The arrows in the small window of the image **(c)** point to striations that are so fine they are barely visible. **(a-c)** © Google, Maxar Technologies.

6.3 Shuraki Kapali Catchment

The following two sections show different glacier detachment related processes and their effects on the Shuraki Kapali catchment. The first section focuses on the glaciated areas and their development after a detachment. Floods resulting from glacier detachment and their effects on downstream settlements are dealt with in the second section.

6.3.1 Glaciated Area

Reference Glacier

The reference glacier in the central subcatchment shows a volume loss of $1.23 \pm 0.09 \times 10^6$ m^3 from 29 October 2014 to 4 September 2022. This corresponds to a melt rate of 0.62 $\pm$0.05 ma^{-1}. From 4 September 2022 to 3 September 2023, the reference glacier shows a volume gain of $0.07 \pm 0.01 \times 10^6$ m^3.

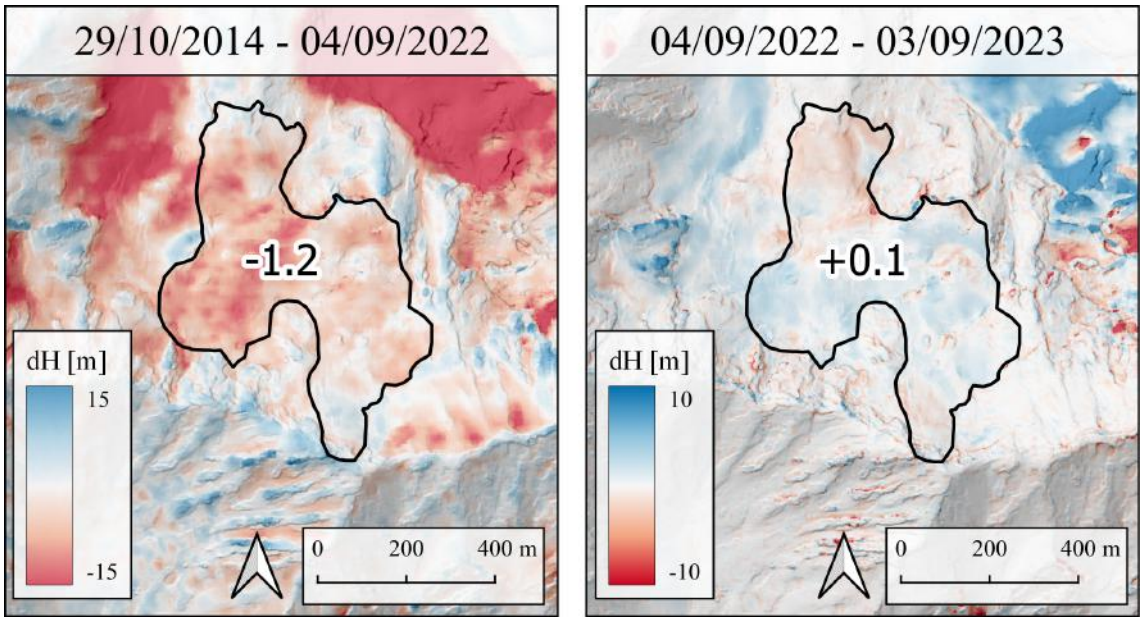

Figure 6.8: DEM differences showing the surface elevation changes of the reference glacier for the two periods 2014-2022 and 2022-2023. The numbers show the volume change in millions of cubic metres. TanDEM-X and Pléiades.

Eastern Subcatchment

Between 10 and 11 July 2017, a large part of the glacier in the western subcatchment detached. This is clearly visible in the DEM difference SK-14/22 (Figure 6.9). As a result, the glacier experienced a massive volume loss of $9.45 \pm 0.13 \times 10^6$ m^3 in the period from 29 October 2014 to 4 September 2022. However, this volume change is not only due to the detachment, but also to climate-induced melting from 2014-2022. Based on the melt rate of the reference glacier during the same period, the change due to melting is estimated to be $-1.54 \pm 0.07 \times 10^6$ m^3. The difference between the total volume change and the change due to melting is $7.9 \pm 0.20 \times 10^6$ m^3 and can be considered as an estimate of the volume of ice that has detached. Since the snow accumulation on the glacier due to avalanches has not been included in the calculation, the $7.9 \pm 0.20 \times 10^6$ m^3 should be regarded as a minimum volume. The DEM difference between 4 September 2022 and 3 September 2023 shows a positive volume change of the glacier of $0.72 \pm 0.01 \times 10^6$ m^3. This corresponds to an average glacier-wide height change of $+3.08 \pm 0.02$ m, which is significantly higher than that of the reference glacier of $+0.29 \pm 0.02$ m during the same period. Due to the proximity of the investigated glacier to the reference glacier, this difference cannot be explained by differences in precipitation. This suggests that other factors, such as avalanches or topographic shielding, must play a decisive role. In addition

to the overall significant increase in volume of the glacier, it is also noticeable that there are clear differences within the glacier. In the upper part, the glacier is losing height (up to -18 m), while in the middle part it is gaining height, in some areas massively (up to +27 m). In the lower part, the glacier also shows a positive change in height, although less pronounced than in the middle section. These results suggest that a surge-like redistribution of mass is taking place. The fact that the glacier was very active during this period can also be seen in the satellite images (Figure A.4). The satellite image of 4 September 2022 shows only a few small crevasses. One year later, on 3 September 2023, the number and length of crevasses had increased significantly. In particular, the upper half of the glacier looks chaotic, with crevasses extending across the entire width of the glacier.

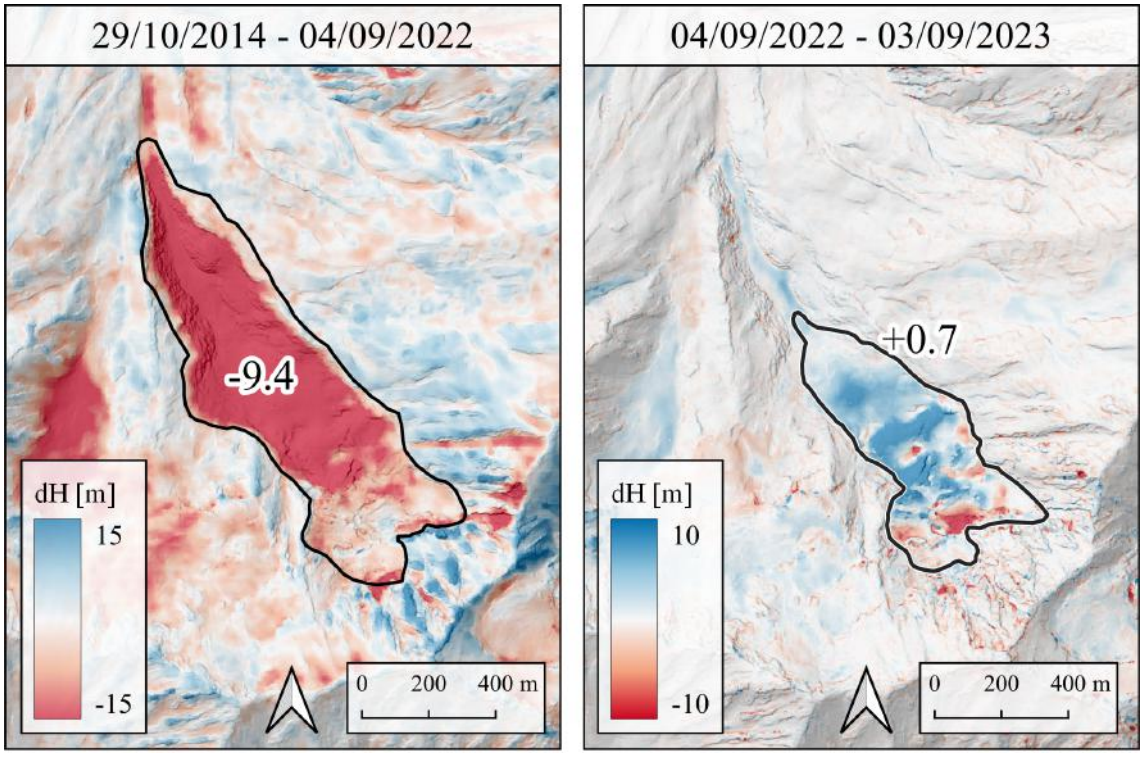

Figure 6.9: Glacier elevation changes during 2014-2022 and 2022-2023 in the eastern Shuraki Kapali subcatchment. The numbers show the volume change in millions of cubic metres within the glacier area. TanDEM-X and Pléiades.

Central Subcatchment

The most recent glacier detachment in the central subcatchment occurred between 13 July and 26 July 2016 (Figure A.5). The lower part of the glacier detached at practically the same elevation as during a glacier detachment in September 2003

(Leinss et al. 2021). A comparison of the glacier's evolution in the years following the two detachments shows strong similarities. Figure 6.10 shows the glacier in 2008 (a), 5 years after the first detachment described in this subcatchment, in 2016 (b), a few days after the second detachment, and in 2022 (c), 6 years after the second detachment. The extent of the lower part of the glacier area is practically congruent in 2008 and 2022. This suggests that the rate of accumulation of snow and ice on the exposed areas was similar after both detachments, at least during the first few years. Whether the accumulation of ice on the exposed areas is due to new ice formation or redistribution of ice cannot be determined from the few DEMs available.

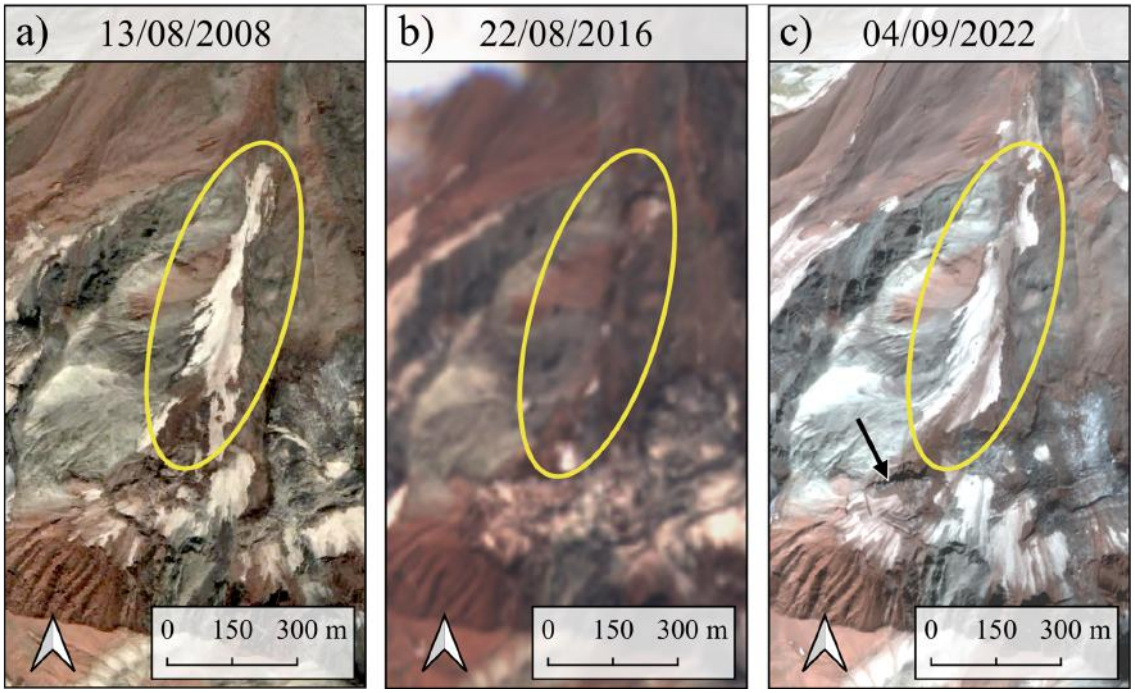

Figure 6.10: Evolution of the glacier in the central subcatchment. The three satellite images show the glacier in 2008 **(a)**, 5 years after the first detachment described in this subcatchment, in 2016 **(b)**, a few days after the second detachment, and in 2022 **(c)**, 6 years after the second detachment. The arrow in the picture on the right points to the triangular glacier part. © Google, Maxar Technologies, **(b)** Copernicus Sentinel data, **(c)** Pléiades.

Interesting developments have also taken place on the glacier above the break-off edge of the 2016 detachment. Of particular interest is the western part of the glacier. It is visually distinct from the rest of the glacier due to its elevated position on a rock outcrop (6.10c). Because of it's triangular shape, it will be referred to as the 'triangular glacier part'. This part of the glacier was connected to the south

by the glacier area that detached in 2016. The detachment exposed the rock band beneath the triangular glacier part. Satellite imagery shows that rockfalls have occurred regularly on this cliff since then, resulting in the formation of a debris cone on the newly forming glacier below. The satellite image of 4 September 2022 shows that the triangular glacier section has two pronounced crevasses in the upper part. A continuous crevasse has formed from these two crevasses, as can be seen in the satellite image of 3 September. In addition to this crevasse, the DEM differences also indicate that the triangular glacier part has moved considerably in recent years. Both the DEM difference SK-14/22 and SK-22/23 show a decrease in height of the glacier in the region above the crevasse and an increase in height at the tip of the triangular glacier part. The widening crevasse and the spatially different changes in elevation indicate a downward movement of the glacier with a resulting mass shift from top to bottom. A plausible explanation for this movement seems to be that the triangular part of the glacier no longer has any counter-pressure at its tip since the detachment. Whether the high rockfall activity in the rock band below the glacier is another cause or a consequence of the glacier advance is difficult to say.

Western Subcatchment

In the western subcatchment there are two glaciers that have been affected by glacier detachments in recent years. One glacier is located at the top of the subcatchment, directly below rock faces, and the other is less than 100 metres further down the valley. On 28 August 2016, large parts of the upper glacier detached and overran the lower glacier (Leinss et al. 2021). Between 21 and 23 June 2019, a large part of the lower glacier then detached (Leinss et al. 2021). Despite their close proximity, the two glaciers reacted very differently to the detachments. The upper glacier did not recover in the years following the detachment. On the contrary, the remnant glacier continued to melt and by 2023 had virtually disappeared. In contrast, the satellite images show that the lower glacier has continuously increased in area since the detachment in 2019. By 2023 it had almost the same area as before the detachment. The different evolution of the two neighbouring glaciers cannot be attributed to different amounts of precipitation due to their proximity. The temperature and the shielding effect do not seem to play a decisive role either, considering that it is the glacier that is higher and under a north-facing rock face that has disappeared. Therefore, it seems plausible that the different evolution of the two glaciers is due to the different input of avalanche snow. This hypothesis is supported by the fact that the lower glacier (22°) has a significantly lower average slope than the upper

glacier (38°), which favours the deposition of avalanche snow. In addition, the lower glacier has a larger catchment area compared to the upper glacier due to its location further down the valley and therefore has a greater change to benefit from avalanche snow.

6.3.2 Runout Zone

The glacier detachments of 28 August 2016 and 10 and 11 July 2017 had an impact reaching as far as the villages of Kapali, Fathobod, Tadzhikabad and the alluvial fan of the Shuraki Kapali river. The Shuraki Kapali river, which normally flows in the gravel field in the centre of the alluvial fan, overflowed its banks on 28 August 2016 as a result of the glacier detachment. The flooding damaged several houses and flooded large areas of the orographic left side of the alluvial fan. The satellite image of 4 September 2016 shows the traces of the flooding, which affected large areas of the orographic left side of the alluvial fan (Figure 6.11b). The same satellite image shows only small traces of erosion on the right-hand side of the alluvial fan, where agricultural land is located. The glacier detachment on 10 and 11 July 2017 again caused flooding, but no houses were damaged this time (Figure 6.11d). In contrast to the flooding of the year before, the orographic right side of the alluvial fan was more affected than the left side. 13.6 ha of fertile land was destroyed by the flooding in 2017 (Figure 6.12). A large part of this land was used for agricultural purposes, as the cultivated fields show (Figure 6.12a). By 2022, the lost farmland had still not been restored, which would not be easy as one of the main branches of the Shuraki Kapali river now runs through the area.

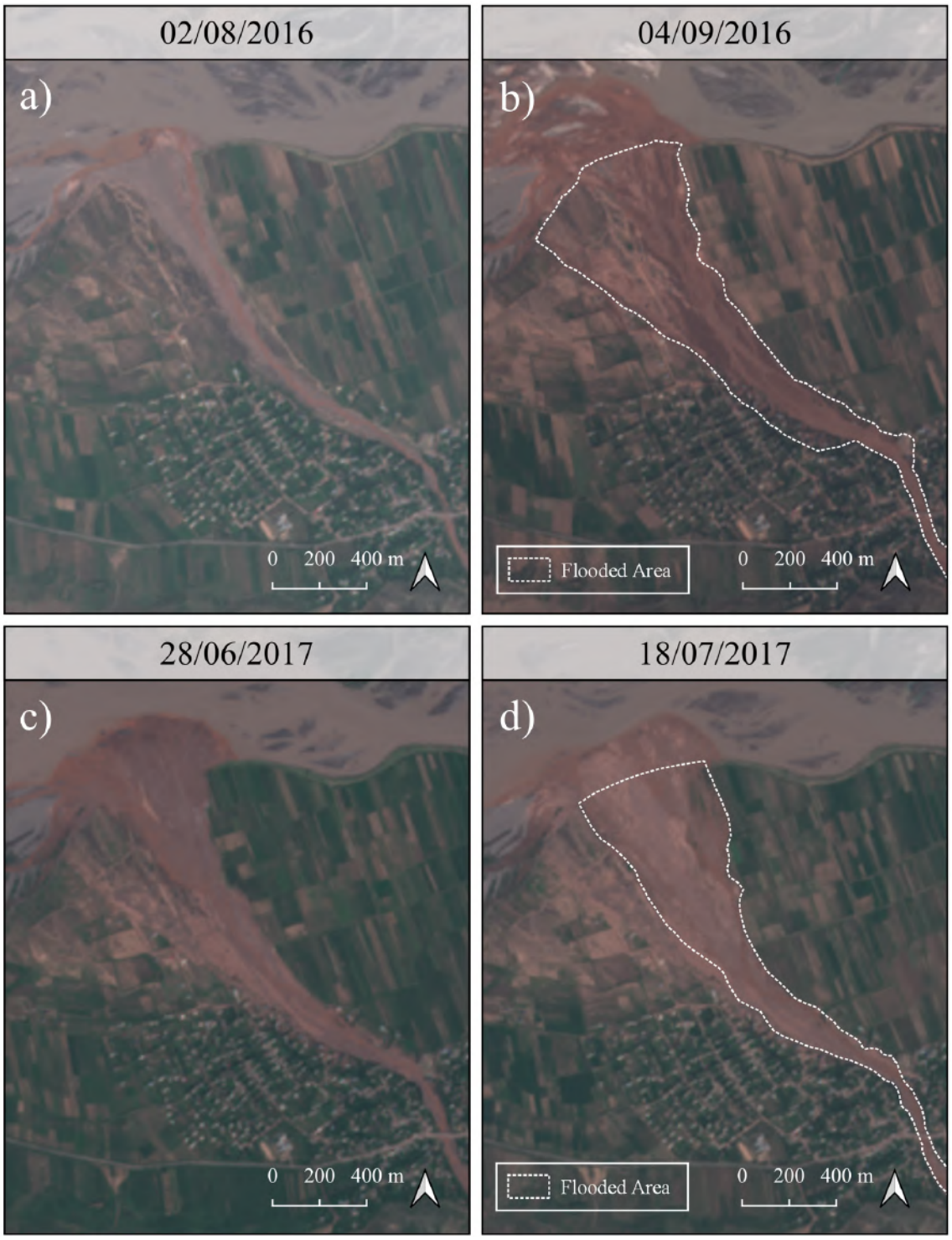

Figure 6.11: Evolution of the alluvial fan of the Shuraki Kapali river. The four figures show the alluvial fan before **(a)** and after **(b)** the flooding in 2016 and before **(c)** and after **(d)** the flooding in 2017. **(a-d)** Copernicus Sentinel data.

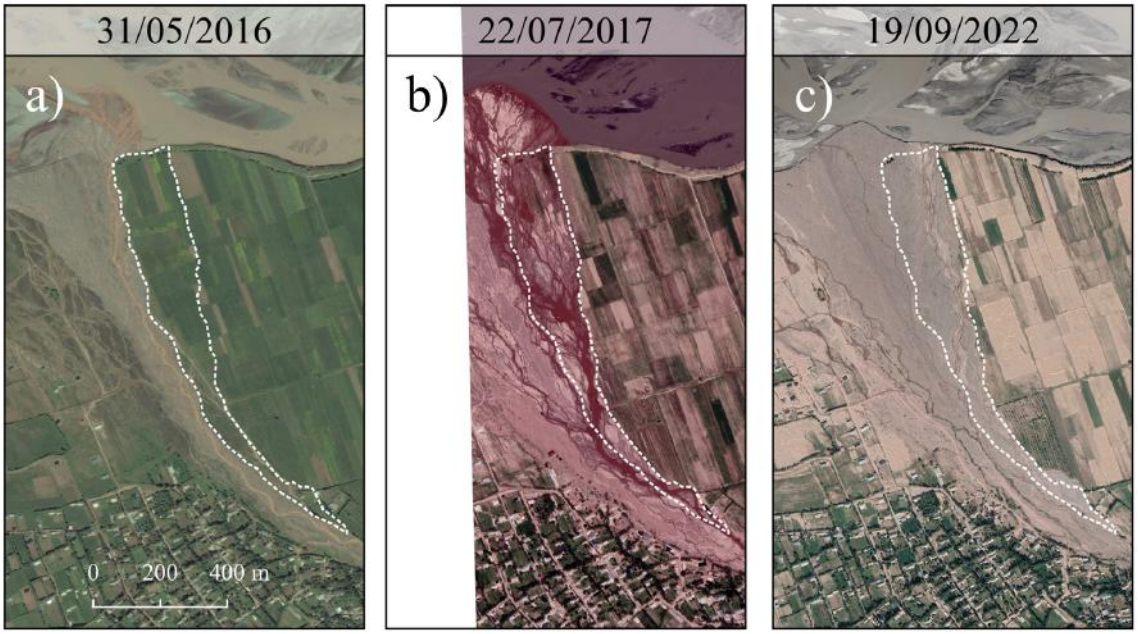

Figure 6.12: Evolution of the orographic right side of the alluvial fan. **(a)** The satellite image shows that the right side of the alluvial fan has been used for agriculture. **(b)** 13.6 ha of fertile land was destroyed by the flooding in 2017. **(c)** By 2023, the destroyed land had not been recultivated. **(a-c)** © Google, Maxar Technologies.

Satellite imagery from 24 September 2016 shows that after the floods of 28 August 2016, a drainage ditch about 1 km long and 25 m wide was dug in the middle of the gravel area up to the mouth of the Surkhob river (Figure 6.13). The ditch was completely filled with debris during the floods of 10/11 July 2017. In June 2021, a new ditch was dug, over 800 metres long and around 15 metres wide. The satellite image of 19 July 2019 shows another protective measure in the lower reaches of the Degilmoni Poyon River. A 100 m long wall (39.114°N, 70.826°E), which did not exist before the two floods, has been built to protect some houses (Figure 6.13). Apart from the ditches and the wall, I could not identify any other protective measures in the satellite images.

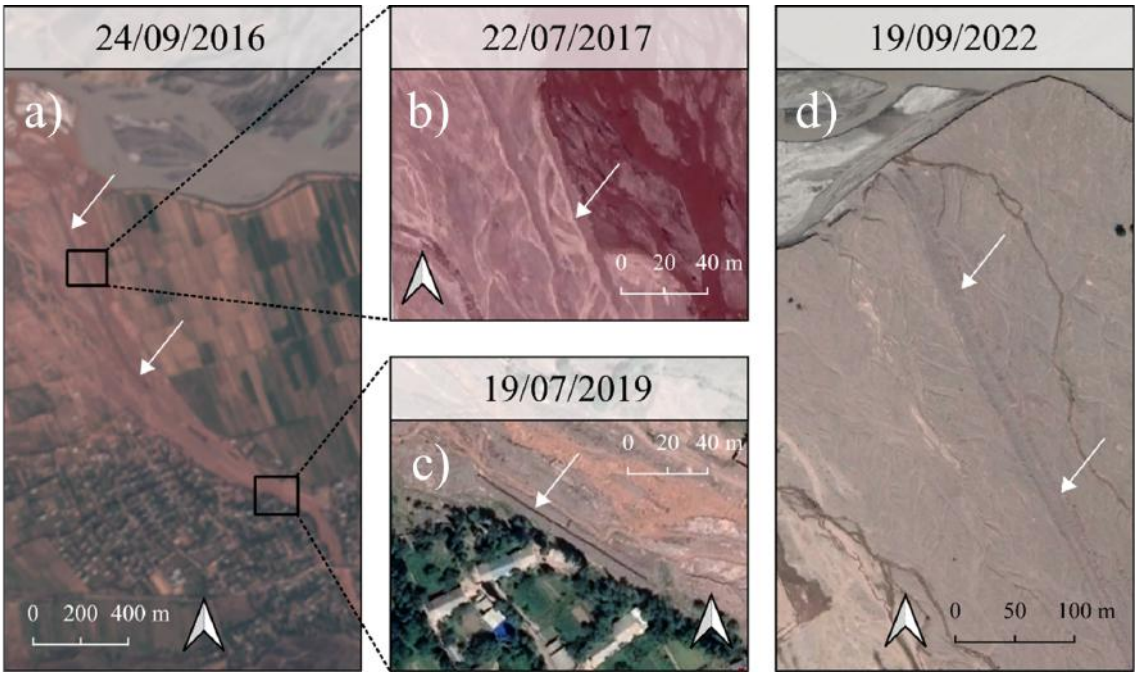

Figure 6.13: Structural measures to prevent flooding in the lower reaches of the Degilmoni Poyon River. **(a)** A drainage ditch was dug after the flooding in 2016 (white arrows). **(b)** Filled drainage ditch after the flooding in 2017. **(c)** A protective wall was built to protect some houses following the floods in 2016 and 2017. **(d)** A new drainage ditch was built in June 2021 (white arrows). **(a)** Copernicus Sentinel data **(b-d)** © Google, Maxar Technologies.

Comparing the number and location of new houses built before and after the floods along the Shuraki Kapali river and on its alluvial fan, there are clear patterns (Figure 6.14). In Fathobod, where no houses were damaged by the floods, some houses were and are still being built close to the river. In the area of the slight left bend of the Shuraki Kapali river, where the 2016 flood damaged houses on both sides of the river, some houses were built before 2016, but none have been built since 2017. Also, no houses have been built since 2017 in the areas of the alluvial fan affected by the floods. However, a new settlement of about 25 houses has been built right next to the area of the alluvial fan that was flooded in 2016. This settlement is located on the part of the alluvial fan where dried-out runoff channels can be seen in the 30 September 2007 satellite image, indicating earlier flooding (Figure A.6).

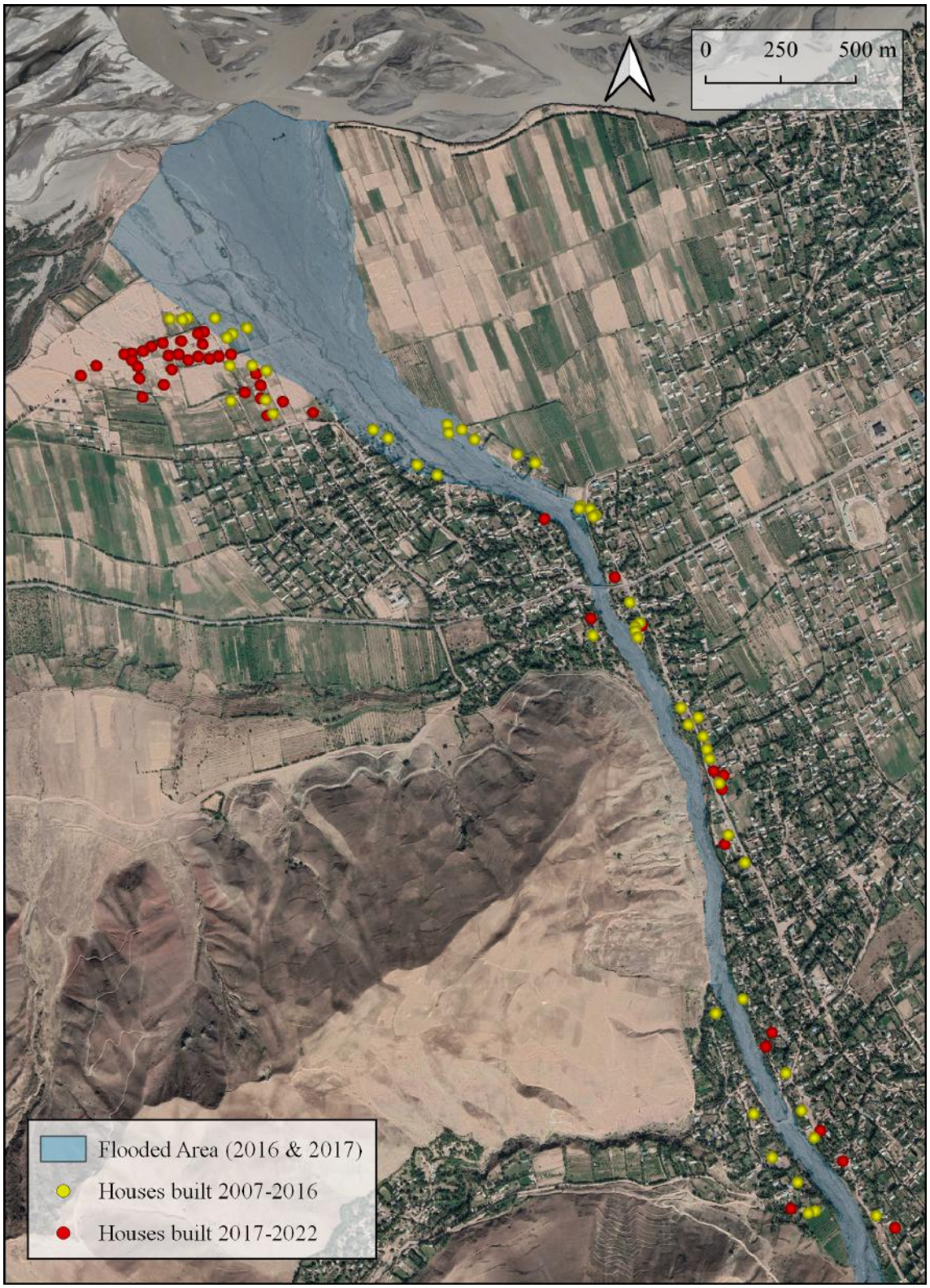

Figure 6.14: Newly built houses along the Shuraki Kapali River before (yellow dots) and after (red dots) the two floods in 2016 and 2017 (blue area). © Google, Maxar Technologies.

7. Discussion

This chapter shows how the new findings from this thesis compare with results from other studies. It further discusses how glacier-related hazards in the Degilmoni Poyon and Shuraki Kapali catchments may develop in the future. Finally, this chapter outlines possible approaches for future research on glacier detachments.

7.1 Comparison to Other Studies

It is not uncommon for glacier beds to be exposed at a time when most glaciers around the world are retreating due to global warming. But what happens to the bed when it is no longer covered by the glacier? A study of the glacier forefield of Griesgletscher showed high erosion rates (5.4 cm a^{-1}), more than 50 times higher than in the rest of the catchment (Delaney et al. 2018). Kääb and Girod (2023) described glacier detachments as a unique natural experiment to provide an indication of the maximum erosion potential that might otherwise be mobilised over longer timescales of gradual glacier retreat. They studied the exposed area of the Sedongpu glacier following a detachment in October 2018 and observed impressive erosion rates. Between December 2018 and 2022, a total volume of about $335 \pm 5 \times 10^6$ m^3 was eroded from the former glacier bed, forming a new canyon up to 300 m deep (Kääb & Girod 2023).

Kääb and Girod (2023) stated that at least some of the other documented detachments are also associated with significant post-detachment erosion activity, with explicit mention of events in Flat Creek and the Petra Pervogo range. Whether the latter refers to the detachments in the Degilmoni Poyon and Shuraki Kapali catchments remains unclear. However, the results of my thesis show that the exposed glacier beds in the Degilmoni Poyon and Shuraki Kapali catchments have not experienced significant erosion, in contrast to the glacier forefield of Griesgletscher and the exposed area of Sedongpu Glacier. This is despite the prevalence of soft, fine-grained and easily erodible lithologies in both catchments (Leinss et al. 2021).

It is likely that this is due to a combination of two factors. First, strong erosion processes do not start immediately after the glacier bed is exposed. For example, the major erosion activity after the Sedongpu event started only three years after the detachment (Kääb & Girod 2023). It has been suggested that this time lag is due to a comparatively stable protective layer covering the weak sediments. This protective layer first had to be eroded by stream erosion before the weak sediments could be mobilised. Second, high erosion rates require that the glacier bed is actually exposed. However, the glaciers in the Degilmoni Poyon and Shuraki Kapali catchments recover very quickly and form ice that protects the originally exposed areas. Just three years after the detachment, the exposed glacier bed in the Degilmoni Poyon catchment was almost completely covered by ice again.
The fact that four out of five glaciers affected by detachments in the Degilmoni Poyon and Shuraki Kapali catchments were able to recover is surprising at first glance. The glaciers analysed in Section 6.1.2, which experienced neither a glacier detachment nor a surge, all showed significant volume losses between 2018 and 2022. This is not surprising as these years were all both warmer and drier than average (cf. Section 6.1.1). Whether the rapid glacier retreat observed in the Petra Pervogo range is just a snapshot or corresponds to the long-term trend cannot be conclusively answered due to a lack of studies. A comparison of the average mass balance of the seven glaciers studied in this thesis with other estimates shows a significantly faster glacier retreat in the period 2018-2022 (Table 7.1). However, the comparison should be treated with caution due to the different scales of the studies.

Table 7.1: Mass balances of glaciers in the Petra Pervogo range and the Pamirs.

Study period	Region	Mass balance [m w.e.yr^{-1}]	Source
1999-2011	Pamir	$+0.14 \pm 0.13$	Gardelle et al. (2013)
2000-2017	Pamir	-0.05 ± 0.06	Li et al. (2022)
2000-2018	Pamir-Alay	-0.32 ± 0.37	Barandun et al. (2021)
2018-2022	Petra Pervogo range	-0.67 ± 0.07	cf. Section 6.1.2

It is not the first time that a glacier has been observed to regain volume following a detachment. The Kolka glacier was also able to regain 40 % of its pre-detachment volume by 2014 after its detachment in 2002 (Petrakov et al. 2018). Nevertheless, the speed at which four of the five affected glaciers in the Degilmoni Poyon and Shuraki Kapali catchments increased in volume is astonishing. As already mentioned, the glacier in the Degilmoni Poyon catchment has reached 35 % of its pre-detachment

volume within three years. The volume increase despite above average temperatures can be attributed to two processes: redistribution of material from the surrounding slopes triggered by the detachment, and accumulation of avalanche snow on the exposed area. The detailed analysis of the exposed area in the Degilmoni Poyon catchment showed that mass redistribution processes triggered by the detachment occurred mainly in the first three years after detachment (September 2019 - September 2022). Primarily ice and snow, but also lithic material was mobilised. Similar redistribution processes were observed after the detachment of the Flat Creek glacier in 2015. There, the so-called debuttressing response resulted in the remaining glacier thinning by an average of 9.2 m, flowing into the emptied trough and causing an average surface elevation increase of 17.7 m (Jacquemart et al. 2022). Another consequence of the debuttressing response was increased rockfall activity and debris accumulation in the release zone of the Flat Creek glacier detachment.

Snow input from avalanches was at least as important for the rapid volume increase of the Degilmoni Poyon glacier as the mass redistribution described above. Other studies have proved that avalanche deposits can strongly influence the mass balance of a glacier. The analysis of three glaciers in the Himalayas (2.4-19.0 km^2), which are all significantly larger than the glaciers analysed in this thesis (0.09-0.63 km^2), shows that extensive avalanches from the headwalls contribute more than 95% of their total accumulation (Laha et al. 2017). This means that both the dynamics and the extent of these glaciers are controlled in the long term by avalanche contributions. Another study, on the Argentière glacier in France (12 km^2), found that avalanches lead to an additional 60% mass accumulation at the base of the headwalls, which corresponds to an additional 20% mass accumulation over the entire glacier (Kneib et al. 2022). The percentage of avalanche deposits relative to solid precipitation accumulation in the exposed areas of the Degilmoni Poyon and Shuraki Kapali catchments cannot be precisely determined from the available data. However, the ratio between the area of the glacier and the area of its surrounding headwalls is significantly smaller in the two catchments studied than for the Argentière glacier. It can therefore be assumed that the difference between additional mass accumulation directly below the headwalls and at the glacier scale is significantly smaller for the glaciers in the Degilmoni Poyon and Shuraki Kapali catchments.

The fact that only four of the five glaciers affected by detachments in the Degilmoni Poyon and Shuraki Kapali catchments are recovering supports the hypothesis that their dynamics and extent are controlled by avalanche contributions. Furthermore, the only glacier that was unable to recover after the detachment was located on a

steep slope with a gradient of 38°, where avalanche snow deposition is very unlikely. The other four glaciers are all located in valleys with average slopes of less than 30 degrees, where avalanche snow deposition is expected.

An exposed glacier bed, which would make it easy to identify a glacier detachment in the landscape, no longer exists in the two catchments studied due to rapid mass accumulation. Looking at the affected glaciers in recent satellite imagery, it is difficult to see that they have experienced a detachment. Traces of glacier detachments in the runout zones also disappear quickly. As described in Section 6.3.2, all of the deposited ice in the Degilmoni Poyon catchment melted within three years after the detachment. In 2024, only two indications can be found in satellite images that point to a glacier detachment in the Degilmoni Poyon catchment. First, there are parallel striations in the first left turn downstream of the glacier. Such striations were also observed after the detachment of Flat Creek glacier (Jacquemart et al. 2022). Second, there are patches of missing vegetation in the runout zone. However, the vegetation has already recovered significantly in the five years since the detachment and will probably soon return to its pre-detachment state. This assumption is also supported by a study of vegetation development after the Kolka event, where the vegetation fully recovered within 10 to 15 years (Leinss et al. 2021). Jacquemart et al. (2022) also identified some small-scale geomorphic and sedimentary signatures of glacier detachments such as molards, kettle-holes or striated rocks in the Flat Creek study. Due to the limited resolution of the satellite imagery, I was unable to assess whether such features are or were also present in the Degilmoni Poyon and Shuraki Kapali catchments. However, as large-scale signatures of glacier detachments seem to disappear relatively quickly, these small-scale features could be of great importance in the identification of past glacier detachments.

7.2 Future Development of Glacier-Related Hazards in the two Study Sites

For repeated detachments from the same glacier to occur, climatic conditions and associated glacier mass balances must allow for the necessary mass accumulation and regrowth (Jacquemart & Cicoira 2022). As discussed above, this is the case for four of the five glaciers analysed in the Degilmoni Poyon and Shuraki Kapali catchments. These glaciers are rapidly regaining volume. If this trend continues, the glaciers may in the future return to (or even exceed) their pre-detachment dimensions. This would mean that there is a risk of these glaciers detaching again in the future.

As past events in the Shuraki Kapali catchment show, it is not uncommon for glaciers to recover from a detachment and detach again. There are glaciers with two documented detachments in all three subcatchments (Leinss et al. 2021). In the Degilmoni Poyon catchment, there is no proof of a glacier detachment before the 2019 event. However, erosion patterns and patches of missing vegetation in the runout zone that are very similar to those of the 2019 event can be seen in satellite imagery prior to 2019 and are possibly the traces of a detachment far back in the past (Leinss et al. 2021).
It is not yet possible to predict if and when further detachments from the glaciers analysed in this thesis will occur. However, the analysis shows that the glaciers are regrowing rapidly. The following two examples indicate that if the glaciers continue to grow at the current rate, they will reach their pre-detachment volume within the next decade. This would mean that further glacier detachments in the Degilmoni Poyon and Shuraki Kapali catchments cannot be ruled out in the coming years:

- In the four years following the detachment in the Degilmoni Poyon catchment, the glacier regained a volume of $3.07 \pm 0.08 \times 10^6$ m^3. This is about one third of the volume lost ($8.72 \pm 0.87 \times 10^6$ m^3). Between September 2022 and September 2023, the glacier grew by $0.66 \pm 0.04 \times 10^6$ m^3 due to avalanche snow deposited on the previously exposed area. Assuming the same climatic conditions as during that period, it would take about nine more years, until 2032, for the glacier to reach the same volume as before the detachment.

- The glacier in the lower part of the central Shuraki Kapali subcatchment had a surprisingly similar extent five years after the first detachment in 2003 and 6 years after the second detachment in 2016. If this regrowth trend continues, the lower part of the glacier will reach more or less the same extent by 2029 as it had before the second detachment in 2016. This does not automatically mean that the lower part of the glacier will detach again, as the history of this glacier shows. The area of the glacier was significantly larger before the detachment in 2003 than before the detachment in 2016.

Two glaciers in the Shuraki Kapali catchment that were particularly active between September 2022 and September 2023 are the triangular glacier in the central subcatchment and the glacier in the eastern subcatchment. The front part of the triangular glacier, which is located on a rock face, is moving downwards. Between September 2022 and September 2023, a crevasse formed, separating the front part, at least superficially, from the rest of the glacier. The front part of the glacier is

relatively small (11.5×10^3 m^2) and would probably not have a major impact on inhabited areas if it were to detach. However, its evolution should be monitored to ensure that there are no people in the area below in case of a detachment.

The glacier in the eastern subcatchment experienced a surge-like redistribution of mass between September 2022 and 2023, resulting in a large number of crevasses on its surface. It is difficult to say whether it is a coincidence or related to the exceptionally high mean annual temperature that the glacier moved so much between the end of 2022 and 2023. However, an earlier study of glacier detachments in the Petra Pervogo range showed that high temperatures are an important factor favoring glacier detachments (Leinss et al. 2021). Compared to the triangular glacier, the glacier in the eastern subcatchment is much larger (225×10^3 m^2). If the entire glacier were to detach from its bed, villages further downstream would likely be affected. It is therefore important that the glacier is monitored so that timely action can be taken in inhabited areas if necessary.

Recent large glacier detachments in the Shuraki Kapali catchment, such as those in 2016 and 2017, overrun the snout of a surging glacier reaching into the main valley further downstream. The glacier snout acts as an obstacle in the runout zone of the glacier detachments, presumably slowing them down. This hypothesis is supported by the satellite image of 22 July 2017 and the DEM difference SK-14/23, both of which show that a lot of material from the glacier detachments was deposited just upstream of the glacier snout. However, the DEM difference SK-14/23 also shows that the surging glacier is in a quiescent phase and is losing volume at its tongue. If this trend continues, the surging glacier may lose considerable length and no longer reach the Shuraki Kapali valley. This would allow detached glacier masses to flow down the valley without having to cross this obstacle, presumably increasing the runout distance of glacier detachments and thus increasing the risk to villages. At the same time, the ice of the glacier snout can be converted into water by frictional heat when it is overrun by detached ice masses. A retreating glacier therefore also means that less water is involved in the processes taking place, reducing the risk to villages. However, it is difficult to assess the overall impact of a possible retreat of the surging glacier on the hazard potential in inhabited areas further down the valley.

As discussed in previous paragraphs, future glacier detachments in the Degilmoni Poyon and Shuraki Kapali catchments cannot be ruled out. Accordingly, further mudflows and flooding as a result of glacier detachments are also possible in the future. However, since the floods of 2016 and 2017, hardly any major structural

measures have been taken in inhabited areas of the Shuraki Kapali catchment to better prepare for such events. Whether organisational measures such as evacuation plans have been taken or early warning systems have been installed cannot be said based on satellite imagery. The analysis of new buildings along the Shuraki Kapali River in the periods of 2007-2016 and 2017-2022 shows that at least no new houses were built in the areas flooded in 2016 and 2017. However, one new settlement was built on the alluvial fan. This is worrying, as a flood of the magnitude of the 2016 event would have just missed it. In addition, satellite imagery from 30 September 2007 shows dried-up erosion rills in the now built-up area. This suggests that floods of greater magnitude than that of 28 August 2016 have occurred in the past. This raises the question of why the alluvial fan is still being built on. A study has shown that flood memory depends on living witnesses and fades away already within two generations and that historical memory is not sufficient to protect human settlements from the consequences of rare catastrophic floods (Fanta, Šálek, & Sklenicka 2019). This underlines the importance of documenting events and their dimensions to pass them on to future generations.

7.3 Future Research on Glacier Detachments

Glacier detachments and the processes involved still raise many questions. This is not surprising, given the recent nature of most documented events. In this section, I discuss approaches to fill the existing research gaps.

Ongoing and future research on glacier detachments can be divided into two categories: Research on the causes of glacier detachments and research on their impacts on the landscape and people. Research on the causes of detachments is the more progressed of the two. However, there is still no precise explanation of the processes leading to glacier detachments. This may be because the knowledge available today is based only on analyses of past glacier detachments. These often occur in remote regions where key data, such as DEMs and meteorological data, are unavailable or of insufficient spatial or temporal resolution. In order to better understand the processes underlying glacier detachments, it would be helpful not only to retrospectively study past events but also to actively build up a measurement network in a test site, where it is possible to follow the processes of a glacier detachment in real time. Test sites have already led to a better understanding of processes for other alpine natural hazards such as debris flows (e.g. Illgraben; Meyrat et al. (2022)) and

avalanches (e.g. Vallée de la Sionne; Sovilla et al. (2008)). The Degilmoni Poyon catchment and in particular the Shuraki Kapali catchment would make an ideal test site. The large number of different detachments in recent decades and the ability of the glaciers to recover from detachments suggest that glacier detachments will continue to occur there in the future. At such a test site, precise meteorological data could be collected using an in-situ meteostation, and repeated high-resolution digital elevation models could be produced using drone surveys or terrestrial laser scanning. The resulting data sets could provide new insights into the glacier dynamics associated with detachments. In addition to targeted monitoring of regions with increased glacier detachment activity, all newly observed glacier detachments need to be documented and analysed. This will make it possible to study how different geographical and climatic conditions affect glacier detachments.

Research on the medium-term landscape impacts of glacier detachments is still very young. Long-term impacts have not yet been studied because of the recent nature of most documented events. Further research on landscape impacts is important to understand how long the different traces of glacier detachments remain visible and how the exposed area evolves. My work has focused on the medium-term landscape impacts of glacier detachments in two specific catchments. It is important to carry out similar studies for other glacier detachments. Ideally, the landscape impacts will be analysed not only by using remote sensing methods but also based on field work. In this way, the variability of landscape responses to glacier detachments can be estimated and similarities between different events can be identified. The Kolka glacier, which detached in 2002, is currently the best case study for analysing the long-term landscape impacts of glacier detachments. In the future, all events whose medium-term impacts have already been analysed will also be suitable for research on long-term impacts. Only if the medium-term effects of glacier retreat on the landscape are known can the long-term effects be clearly distinguished from the medium-term impacts.

In addition to detailed analysis of individual glacier detachments, it is important to establish an ongoing inventory of all documented events. This makes it possible to analyse whether the frequency of glacier detachments is increasing, staying the same or decreasing on a regional or global scale over time. This knowledge may be important for assessing the impact of climate change on glacier detachments, and thus for natural hazard management. Effective natural hazard management also requires research in two other areas: How can glacier detachments be detected at an early stage, and what structural and organisational measures can be taken to

minimise the impact of a glacier detachment on inhabited areas? Answering these two questions would allow early action to be taken in the downstream villages and reduce the potential for damage.

8. Conclusion

Using remote sensing imagery, I analysed the medium-term impacts of catastrophic glacier detachments in the Degilmoni Poyon and Shuraki Kapali catchments, and then compared these findings with other studies to place them in a broader context. Based on the knowledge gained from this analysis, I answered the three research questions as follows:

How do glaciers and exposed glacier beds evolve after catastrophic glacier detachments?

Four out of five glaciers in the Degilmoni Poyon and Shuraki Kapali catchments that lost a large part of their volume due to a detachment between 2016 and 2019 were able to regain mass by 2023. This was despite the fact that the period from 2016 to 2022 was both warmer and drier than average. All of the glaciers that are recovering are located in a valley with a relatively low slope ($<30°$). The only glacier, which did not recover after the detachment, is located on a very steep and plane slope (38°). The correlation between the slope of glaciers and their ability to recover after detachment appears to be due to avalanching. Glaciers with a low average slope are fed by avalanches, allowing them to maintain a positive mass balance during the study period. The detailed analysis of the exposed area in the Degilmoni Poyon catchment has shown that the glacier regained a third of its pre-detachment volume between 2019 and 2023. At least half of the increase in volume can be explained by avalanching. The other half is due to mass redistribution processes triggered by the detachment, whereby mainly ice, but to a lesser extent also lithic material from the surrounding slopes, was deposited in the exposed area. Due to the rapid recovery of the glacier, the exposed glacier bed was covered by ice again within a few years. As a result, no significant erosion was observed. An other study of Sedongpu glacier has shown that the glacier bed can also evolve very differently after being exposed by a detachment. In the case of Sedongpu, the glacier was unable to recover after

the detachment, leaving the glacier bed exposed and resulting in enormous rates of erosion. The comparison of these two studies leads to the conclusion that the erosion activity within an exposed area is determined by the ability of a glacier to recover. Glacier detachments only occur where soft, fine-grained sediments are present. If these sediments are not protected by a glacier, high rates of erosion can be expected.

What traces does a glacier detachment leave in its runout zone and how long do they remain visible?

In the runout zone of the Degilmoni Poyon catchment, $7.57 \pm 2.20 \times 10^6$ m^3 of predominantly ice was deposited as a result of the detachment in 2019. Three years after the detachment, in 2022, all the ice had already melted and thus the most obvious feature of a glacier detachment had already disappeared from the landscape. The destructive impact of the glacier detachment on vegetation lasts longer. In 2024, there are still missing patches where the vegetation has not yet been able to recover. However, it seems to be only a matter of a few years before this trace also disappears, considering two points: First, many of the areas where vegetation was destroyed by the detachment have already been recolonised by 2024. Second, it took just over 10 years for vegetation to fully recover after the detachment of the Kolka glacier in the North Caucasus. Other characteristic features of glacier detachments still visible in 2024 are parallel striations. Small-scale signatures of the glacier detachment, such as molards, kettle-holes or striated rocks, could not be assessed due to the limited spatial resolution of the satellite imagery. As large-scale signs of glacier detachments tend to fade relatively quickly, these small-scale features could potentially play a crucial role in identifying past glacier detachments

What are the impacts of glacier detachments on anthropogenic landscapes, and what adaptation measures are being taken to counteract them?

Two detachments in 2016 and 2017 led to mudflows/floods that affected the villages of Kapali, Fathobod, Tadzhikabad and the alluvial fan of the Shuraki Kapali river. Houses were damaged and a total of 13.6 ha of fertile land was destroyed. In comparison to other documented glacier detachments, particularly those of the Kolka glacier and the Aru twin glaciers, which claimed many lives, the damage in the Shuraki Kapali catchment was relatively limited. Neretheless, some structural protection measures have been taken. After the first flood in 2016, a drainage ditch

was dug in the middle of the gravel area all the way to the mouth of the Surkhob river. This ditch was refilled by the event a year later. A new ditch was dug in 2021. In addition, a 100 m long wall was built after the two floods to protect some houses. Whether organisational measures such as evacuation plans have been taken or early warning systems have been installed cannot be said based on satellite imagery. The floods also had an impact on construction activities along the Shuraki Kapali river. In areas where no houses were damaged by the floods, new houses were also built after 2017, but no new houses were built in flood-affected areas. However, a new settlement was built on the alluvial fan in an area just missed by the flood in 2016. Given the potential for further glacier detachments in the Shuraki Kapali catchment, this settlement development should be viewed critically.

Bibliography

Alean, J. (1985). Ice Avalanches: Some Empirical Information about their Formation and Reach. *Journal of Glaciology*, *31*(109), 324–333. https://doi.org/10.3189/s0022143000006663

Barandun, M., Pohl, E., Naegeli, K., McNabb, R., Huss, M., Berthier, E., Saks, T., & Hoelzle, M. (2021). Hot Spots of Glacier Mass Balance Variability in Central Asia. *Geophysical Research Letters*, *48*(11). https://doi.org/10.1029/2020GL092084

Berthier, E., Larsen, C., Durkin, W. J., Willis, M. J., & Pritchard, M. E. (2018, April). Brief communication: Unabated wastage of the Juneau and Stikine icefields (southeast Alaska) in the early 21st century. https://doi.org/10.5194/tc-12-1523-2018

Berthier, E., Lebreton, J., Fontannaz, D., Hosford, S., Belart, J. M. C., Brun, F., Andreassen, L. M., Menounos, B., & Blondel, C. (2024). The Pléiades Glacier Observatory: high resolution digital elevation models and ortho-imagery to monitor glacier change. https://doi.org/10.5194/egusphere-2024-250

Calvin, K., Dasgupta, D., Krinner, G., Mukherji, A., Thorne, P. W., Trisos, C., Romero, J., Aldunce, P., Barrett, K., Blanco, G., Cheung, W. W., Connors, S., Denton, F., Diongue-Niang, A., Dodman, D., Garschagen, M., Geden, O., Hayward, B., Jones, C., ... Ha, M. (2023, July). *IPCC, 2023: Climate Change 2023: Synthesis Report. Contribution of Working Groups I, II and III to the Sixth Assessment Report of the Intergovernmental Panel on Climate Change [Core Writing Team, H. Lee and J. Romero (eds.)]. IPCC, Geneva, Switzerland.* (P. Arias, M. Bustamante, I. Elgizouli, G. Flato, M. Howden, C. Méndez-Vallejo, J. J. Pereira, R. Pichs-Madruga, S. K. Rose, Y. Saheb, R. Sánchez Rodríguez, D. Ürge-Vorsatz, C. Xiao, N. Yassaa, J. Romero, J. Kim, E. F. Haites, Y. Jung, R. Stavins, ... C. Péan, Eds.; tech. rep.). Intergovernmental Panel on Climate Change. https://doi.org/10.59327/IPCC/AR6-9789291691647

Casey, J. A., Howell, S. E., Tivy, A., & Haas, C. (2016). Separability of sea ice types from wide swath C- and L-band synthetic aperture radar imagery acquired during the melt season. *Remote Sensing of Environment*, *174*, 314–328. https://doi.org/10.1016/j.rse.2015.12.021

Delaney, I., Bauder, A., Huss, M., & Weidmann, Y. (2018). Proglacial erosion rates and processes in a glacierized catchment in the Swiss Alps. *Earth Surface Processes and Landforms*, *43*(4), 765–778. https://doi.org/10.1002/esp.4239

Deschamps-Berger, C., Gascoin, S., Berthier, E., Deems, J., Gutmann, E., Dehecq, A., Shean, D., & Dumont, M. (2020). Snow depth mapping from stereo satellite imagery in mountainous terrain: Evaluation using airborne laser-scanning data. *Cryosphere*, *14*(9), 2925–2940. https://doi.org/10.5194/tc-14-2925-2020

Du Pasquier, L. (1896). L'avalanche du glacier de l'Altels le 11 septembre 1895. *Annales de Géographie*, *5*(23), 458–468. https://doi.org/10.3406/geo.1896.5954

Evans, S. G., & Delaney, K. B. (2015). Catastrophic Mass Flows in the Mountain Glacial Environment. In *Snow and ice-related hazards, risks, and disasters* (pp. 563–606). Elsevier Inc. https://doi.org/10.1016/B978-0-12-394849-6.00016-0

Evans, S. G., Tutubalina, O. V., Drobyshev, V. N., Chernomorets, S. S., McDougall, S., Petrakov, D. A., & Hungr, O. (2009). Catastrophic detachment and high-velocity long-runout flow of Kolka Glacier, Caucasus Mountains, Russia in 2002. *Geomorphology*, *105*(3-4), 314–321. https://doi.org/10.1016/j.geomorph.2008.10.008

Fanta, V., Šálek, M., & Sklenicka, P. (2019). How long do floods throughout the millennium remain in the collective memory? *Nature Communications*, *10*(1). https://doi.org/10.1038/s41467-019-09102-3

Gardelle, J., Berthier, E., Arnaud, Y., & Kääb, A. (2013). Region-wide glacier mass balances over the Pamir-Karakoram-Himalaya during 1999–2011. *Cryosphere*, *7*(4), 1263–1286. https://doi.org/10.5194/tc-7-1263-2013

Gdulová, K., Marešová, J., & Moudrý, V. (2020). Accuracy assessment of the global TanDEM-X digital elevation model in a mountain environment. *Remote Sensing of Environment*, *241*. https://doi.org/10.1016/j.rse.2020.111724

Gilbert, A., Leinss, S., Kargel, J., Kääb, A., Yao, T., Gascoin, S., Leonard, G., Berthier, E., & Karki, A. (2018). Mechanisms leading to the 2016 giant twin glacier collapses, Aru range, Tibet. https://doi.org/10.5194/tc-2018-45

Goerlich, F., Bolch, T., & Paul, F. (2020). More dynamic than expected: An updated survey of surging glaciers in the Pamir. *Earth System Science Data*, *12*(4), 3161–3176. https://doi.org/10.5194/essd-12-3161-2020

Guth, P. L., Van Niekerk, A., Grohmann, C. H., Muller, J. P., Hawker, L., Florinsky, I. V., Gesch, D., Reuter, H. I., Herrera-Cruz, V., Riazanoff, S., López-Vázquez, C., Carabajal, C. C., Albinet, C., & Strobl, P. (2021). Digital elevation models: Terminology and definitions. *Remote Sensing*, *13*(18). https://doi.org/10.3390/rs13183581

Haeberli, W., Huggel, C., Kääb, A., Zgraggen-Oswald, S., Polkvoj, A., Galushkin, I., Zotikov, I., & Osokin, N. (2004). The Kolka-Karmadon rock/ice slide of 20 September 2002: An extraordinary event of historical dimensions in North Ossetia, Russian Caucasus. *Journal of Glaciology*, *50*(171), 533–546. https://doi.org/10.3189/172756504781829710

Harrison, W. D., & Post, A. S. (2003). How much do we really know about glacier surging? *Annals of Glaciology*, *36*, 1–6. https://doi.org/10.3189/172756403781816185

Huggel, C., Zgraggen-Oswald, S., Haeberli, W., Kääb, A., Polkvoj, A., Galushkin, I., & Evans, S. G. (2005). The 2002 rock/ice avalanche at Kolka/Karmadon, Russian Caucasus: Assessment of extraordinary avalanche formation and mobility, and application of QuickBird satellite imagery. *Natural Hazards and Earth System Science*, *5*(2), 173–187. https://doi.org/10.5194/nhess-5-173-2005

Huss, M. (2013). Density assumptions for converting geodetic glacier volume change to mass change. *The Cryosphere*, *7*(3), 877–887. https://doi.org/10.5194/tc-7-877-2013

Jacquemart, M. (2019). DEMDiff_UncertaintyEstimate. https://github.com/mjacqu/FlatCreekProject/blob/master/DEMDiff_UncertaintyEstimate.py

Jacquemart, M., & Cicoira, A. (2022). Hazardous Glacier Instabilities: Ice Avalanches, Sudden Large-Volume Detachments of Low-Angle Mountain Glaciers, and Glacier Surges. *Treatise on Geomorphology*, *500*, 330–345. https://doi.org/10.1016/B978-0-12-818234-5.00188-7

Jacquemart, M., Loso, M., Leopold, M., Welty, E., Berthier, E., Hansen, J. S., Sykes, J., & Tiampo, K. (2020). What drives large-scale glacier detachments? Insights from Flat Creek glacier, St. Elias Mountains, Alaska. *Geology*, *48*(7), 703–707. https://doi.org/10.1130/G47211.1

Jacquemart, M., Welty, E., Leopold, M., Loso, M., Lajoie, L., & Tiampo, K. (2022). Geomorphic and sedimentary signatures of catastrophic glacier detachments: A first assessment from Flat Creek, Alaska. *Geomorphology*, *414*. https://doi.org/10.1016/j.geomorph.2022.108376

Jacquemart Mylène. (2023). personal communication.

Jacquet, J., McCoy, S. W., McGrath, D., Nimick, D. A., Fahey, M., O'kuinghttons, J., Friesen, B. A., & Leidich, J. (2017). Hydrologic and geomorphic changes resulting from episodic glacial lake outburst floods: Rio Colonia, Patagonia, Chile. *Geophysical Research Letters*, *44*(2), 854–864. https://doi.org/10.1002/2016GL071374

James, L. A., Hodgson, M. E., Ghoshal, S., & Latiolais, M. M. (2012). Geomorphic change detection using historic maps and DEM differencing: The temporal dimension of geospatial analysis. *Geomorphology*, *137*(1), 181–198. https://doi.org/10.1016/j.geomorph.2010.10.039

Jouberton, A. P. (2024). personal communication.

Kääb, A., & Girod, L. (2023). Brief communication: Rapid
335 x 10 6 m3 bed erosion after detachment of the Sedongpu Glacier (Tibet). *The Cryosphere*, *17*(6), 2533–2541. https://doi.org/10.5194/tc-17-2533-2023

Kääb, A., Jacquemart, M. n., Gilbert, A., Leinss, S., Girod, L., Huggel, C., Falaschi, D., Ugalde, F., Petrakov, D., Chernomorets, S., Dokukin, M., Paul, F., Gascoin, S., Berthier, E., & S. Kargel, J. (2021). Sudden large-volume detachments of low-angle mountain glaciers - More frequent than thought? *Cryosphere*, *15*(4), 1751–1785. https://doi.org/10.5194/tc-15-1751-2021

Kääb, A., Leinss, S., Gilbert, A., Bühler, Y., Gascoin, S., Evans, S. G., Bartelt, P., Berthier, E., Brun, F., Chao, W. A., Farinotti, D., Gimbert, F., Guo, W., Huggel, C., Kargel, J. S., Leonard, G. J., Tian, L., Treichler, D., & Yao, T. (2018). Massive collapse of two glaciers in western Tibet in 2016 after surge-like instability. *Nature Geoscience*, *11*(2), 114–120. https://doi.org/10.1038/s41561-017-0039-7

Kneib, M., Dehecq, A., Gilbert, A., Basset, A., Miles, E. S., Jouvet, G., Jourdain, B., Ducasse, E., Beraud, L., Rabatel, A., Mouginot, J., Carcanade, G., Laarman, O., Brun, F., & Six, D. (2022). Distributed surface mass balance of an avalanche-fed glacier. https://doi.org/10.5194/egusphere-2024-1733

Kotlyakov, V. M., Rototaeva, O. V., & Nosenko. (2004). The September 2002 Kolka Glacier Catastrophe in North Ossetia, Russian Federation: Evidence and Analysis. *Mountain Research and Development*, *24*(1), 78–83. https://doi.org/10.1659/0276

Kubanek, J., Poland, M. P., & Biggs, J. (2021). Applications of bistatic radar to volcano topography-a review of ten years of TanDEM-X. *IEEE Journal of Selected Topics in Applied Earth Observations and Remote Sensing*, *14*, 3282–3302. https://doi.org/10.1109/JSTARS.2021.3055653

Kumar, G., Chan, Y. C., Sun, C. W., & Chen, C. T. (2024). Decadal-scale assessment of sediment denudation rates in the Zhoukou River Basin, Taiwan: insights from improved DEMs

of differencing based on spectral analysis. *Geomatics, Natural Hazards and Risk*, *15*(1). https://doi.org/10.1080/19475705.2024.2363428

Laha, S., Kumari, R., Singh, S., Mishra, A., Sharma, T., Banerjee, A., Nainwal, H. C., & Shankar, R. (2017). Evaluating the contribution of avalanching to the mass balance of Himalayan glaciers. *Annals of Glaciology*, *58*(75), 110–118. https://doi.org/10.1017/aog.2017.27

Leinss, S. (2023). personal communication.

Leinss, S., Bernardini, E., Jacquemart, M., & Dokukin, M. (2021). Glacier detachments and rock-ice avalanches in the Petra Pervogo range, Tajikistan (1973-2019). *Natural Hazards and Earth System Sciences*, *21*(5), 1409–1429. https://doi.org/10.5194/nhess-21-1409-2021

Li, Z., Wang, N., Chen, A., Liang, Q., & Yang, D. Q. (2022). Slight change of glaciers in the Pamir over the period 2000â2017. *Arctic, Antarctic, and Alpine Research*, *54*(1), 13–24. https://doi.org/10.1080/15230430.2022.2028475

Mannerfelt, E., Hugonnet, R., & Dehecq, A. (2021). xDEM. https://xdem-erikm.readthedocs.io/en/latest/index.html

Marti, R., Gascoin, S., Berthier, E., De Pinel, M., Houet, T., & Laffly, D. (2016). Mapping snow depth in open alpine terrain from stereo satellite imagery. *Cryosphere*, *10*(4), 1361–1380. https://doi.org/10.5194/tc-10-1361-2016

Meier, M. F., & Post, A. (1969). What are glacier surges? *Canadian Journal of Earth Sciences*, *6*(4), 807–817. https://doi.org/https://doi.org/10.1139/e69-081

Meyrat, G., McArdell, B., Ivanova, K., Müller, C., & Bartelt, P. (2022, February). A dilatant, two-layer debris flow model validated by flow density measurements at the Swiss illgraben test site. https://doi.org/10.1007/s10346-021-01733-2

Miles, E. S. (2023). personal communication.

Mukherjee, S., Joshi, P. K., Mukherjee, S., Ghosh, A., Garg, R. D., & Mukhopadhyay, A. (2012). Evaluation of vertical accuracy of open source Digital Elevation Model (DEM). *International Journal of Applied Earth Observation and Geoinformation*, *21*(1), 205–217. https://doi.org/10.1016/j.jag.2012.09.004

Nuth, C., & Kääb. (2011). Co-registration and bias corrections of satellite elevation data sets for quantifying glacier thickness change. *Cryosphere*, *5*(1), 271–290. https://doi.org/10.5194/tc-5-271-2011

Obu, J., Westermann, S., Bartsch, A., Berdnikov, N., Christiansen, H. H., Dashtseren, A., Delaloye, R., Elberling, B., Etzelmüller, B., Kholodov, A., Khomutov, A., Kääb, A., Leibman, M. O., Lewkowicz, A. G., Panda, S. K., Romanovsky, V., Way, R. G., Westergaard-Nielsen, A., Wu, T., … Zou, D. (2019, June). Northern Hemisphere permafrost map based on TTOP modelling for 2000â2016 at 1â¯km2 scale. https://doi.org/10.1016/j.earscirev.2019.04.023

Pamir Project. (2022). Pamir Project. https://pamir-project.ch/

Paul, F., Bolch, T., Kääb, A., Nagler, T., Nuth, C., Scharrer, K., Shepherd, A., Strozzi, T., Ticconi, F., Bhambri, R., Berthier, E., Bevan, S., Gourmelen, N., Heid, T., Jeong, S., Kunz, M., Lauknes, T. R., Luckman, A., Merryman Boncori, J. P., … Van Niel, T. (2015). The glaciers climate change initiative: Methods for creating glacier area, elevation change and velocity products. *Remote Sensing of Environment*, *162*, 408–426. https://doi.org/10.1016/j.rse.2013.07.043

Petrakov, D. A., Aristov, K. A., Aleynikov, A. A., Boyko, E. S., Drobyshev, V. N., Kovalenko, N. V., Tutubalina, O. V., & Chernomorets, S. S. (2018). Rapid regeneration of the kolka

glacier (caucasus) after the 2002 glacial disaster. *Earth's Cryosphere*, *22*(1), 58–71. https://doi.org/10.21782/KZ1560-7496-2018-1(58-71)

Phiri, D., Simwanda, M., Salekin, S., Nyirenda, V. R., Murayama, Y., & Ranagalage, M. (2020, July). Sentinel-2 data for land cover/use mapping: A review. https://doi.org/10.3390/rs12142291

Post, A. (1969). Distribution of Surging Glaciers in Western North America. *Journal of Glaciology*, *8*(53), 229–240. https://doi.org/10.3189/s0022143000031221

Pralong, A., & Funk, M. (2006). On the instability of avalanching glaciers. *Journal of Glaciology*, *52*(176), 31–48. https://doi.org/10.3189/172756506781828980

Prokešová, R., Kardoš, M., Tábořík, P., Medvedová, A., Stacke, V., & Chudý, F. (2014). Kinematic behaviour of a large earthflow defined by surface displacement monitoring, DEM differencing, and ERT imaging. *Geomorphology*, *224*, 86–101. https://doi.org/10.1016/j.geomorph.2014.06.029

QGIS. (2024). GDAL analysis. https://docs.qgis.org/2.18/en/docs/user_manual/processing_algs/gdalogr/gdal_analysis.html#fill-nodata

RGI 7.0 Consortium. (2023). *Randolph Glacier Inventory - A Dataset of Global Glacier Outlines, Version 7.0* (tech. rep.). NSIDC: National Snow and Ice Data Center. Boulder, Colorado USA. https://doi.org/doi:10.5067/f6jmovy5navz

Sevestre, H., & Benn, D. I. (2015). Climatic and geometric controls on the global distribution of surge-type glaciers: Implications for a unifying model of surging. *Journal of Glaciology*, *61*(228), 646–662. https://doi.org/10.3189/2015JoG14J136

Sovilla, B., Schaer, M., Kern, M., & Bartelt, P. (2008). Impact Pressures and flow regimes in dense snow avalanches observed at the Vallée de la Sionne test site. *Journal of Geophysical Research: Earth Surface*, *113*(1). https://doi.org/10.1029/2006JF000688

Steiner, J. F., Kraaijenbrink, P. D., Jiduc, S. G., & Immerzeel, W. W. (2018, January). Brief communication: The Khurdopin glacier surge revisited - Extreme flow velocities and formation of a dammed lake in 2017. https://doi.org/10.5194/tc-12-95-2018

Williams, R. D. (2012). *DEMs of Difference* (tech. rep.). Institute of Geography and Earth Science, Aberystwyth University.

WMO. (2017a). *Technical regulations* (Vol. WMO-No. 49). World Meteorological Organization.

WMO. (2017b). *WMO Guidelines on the Calculation of Climate Normals* (tech. rep.).

Zhao, J., & Floricioiu, D. (2017). The penetration effects on TanDEM-X elevation using the GNSS and laser altimetry measurements in Antarctica. *International Archives of the Photogrammetry, Remote Sensing and Spatial Information Sciences - ISPRS Archives*, *42*(2W7), 1593–1600. https://doi.org/10.5194/isprs-archives-XLII-2-W7-1593-2017

Zou, C., Jansen, J. D., Carling, P. A., Dou, X., Wei, Z., & Fan, X. (2023). Triggers for multiple glacier detachments from a low-angle valley glacier in the Amney Machen Range, eastern Tibetan Plateau. *Geomorphology*, *440*. https://doi.org/10.1016/j.geomorph.2023.108867

A. Appendix

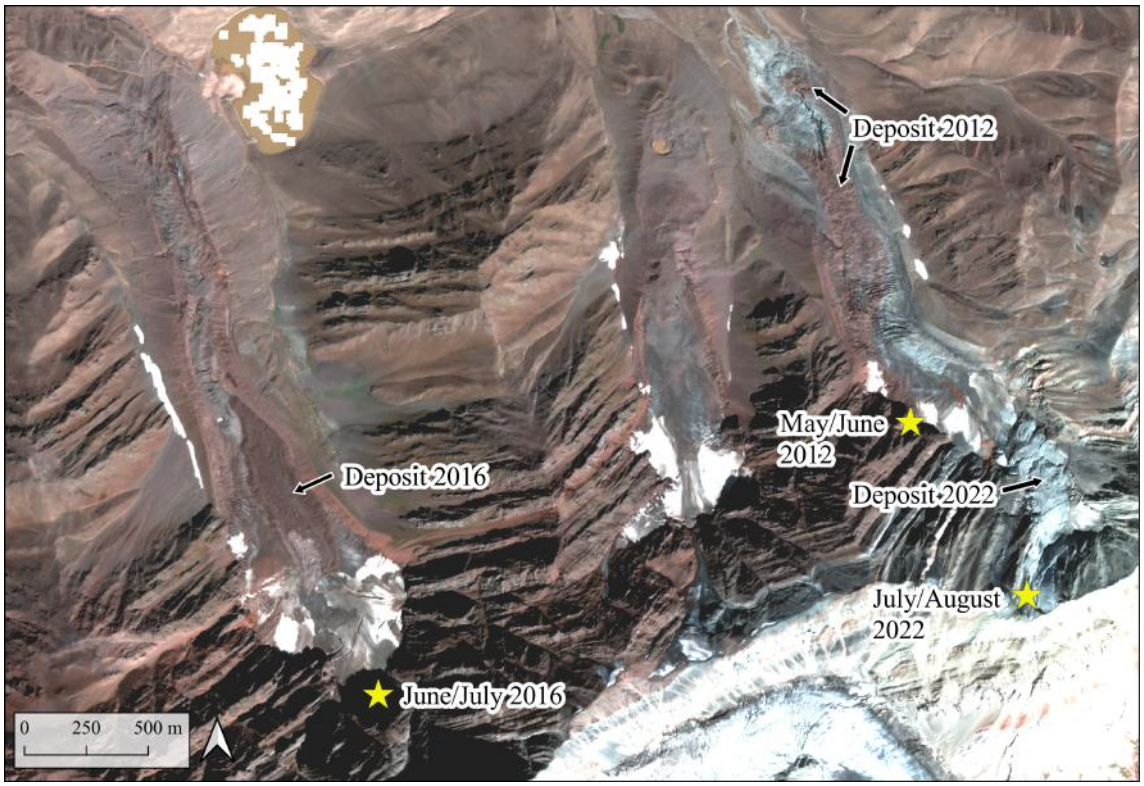

Figure A.1: Overview over the two glacier surges potentially induced by rockfall events onto the glacier. The yellow stars show where the rockfalls originated. Pléiades.

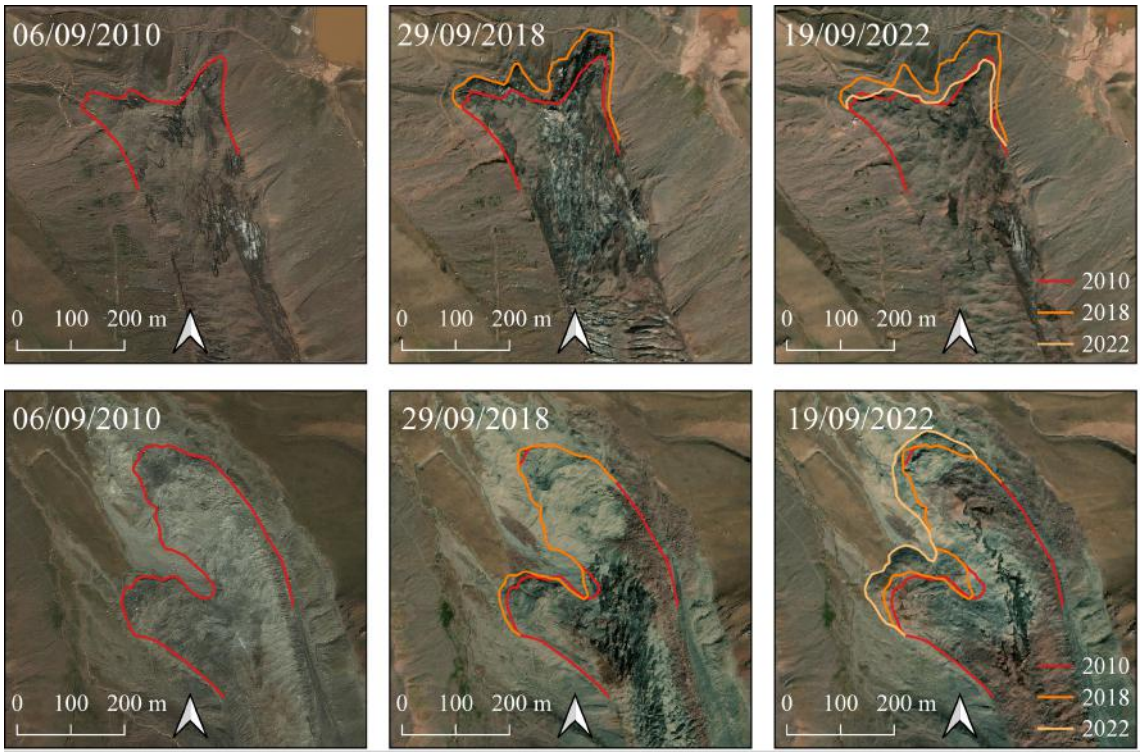

Figure A.2: The upper row shows the changes in length of the surging glacier in 39.024°N, 70.866°E and the lower row those of the surging glacier in 39.021°N, 70.899°E. © Google, Maxar Technologies.

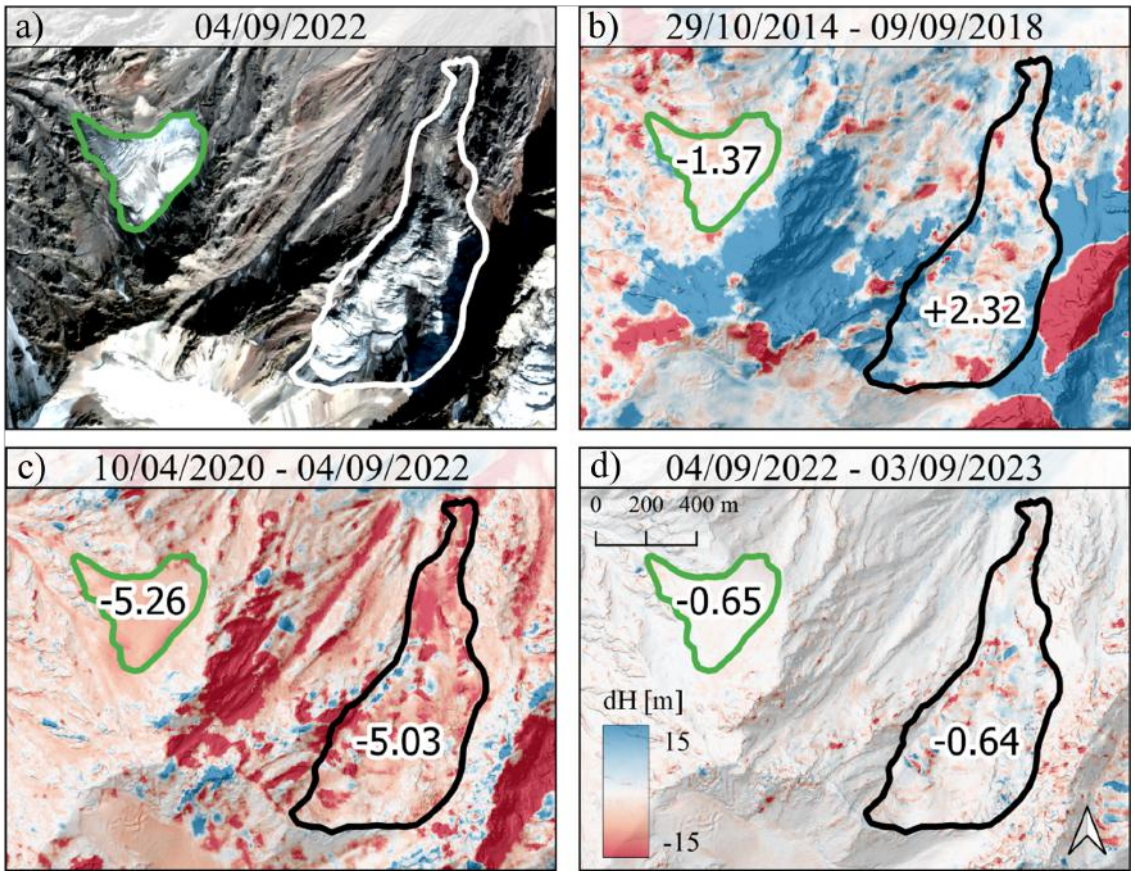

Figure A.3: Comparison of mean surface elevation change of the glacier above the exposed area in the Degilmoni Poyon catchment with a neighbouring glacier. **(a)** Satellite image. **(b)** DEM difference DP-14/18, which contains a number of artefacts. **(c, d)** In the DEM differences DP-20/22 and DP-22/23, the two glaciers show similar elevation changes. **(a, d)** Pléiades, **(b)** TanDEM-X, WorldView, **(c)** WorldView, Pléiades.

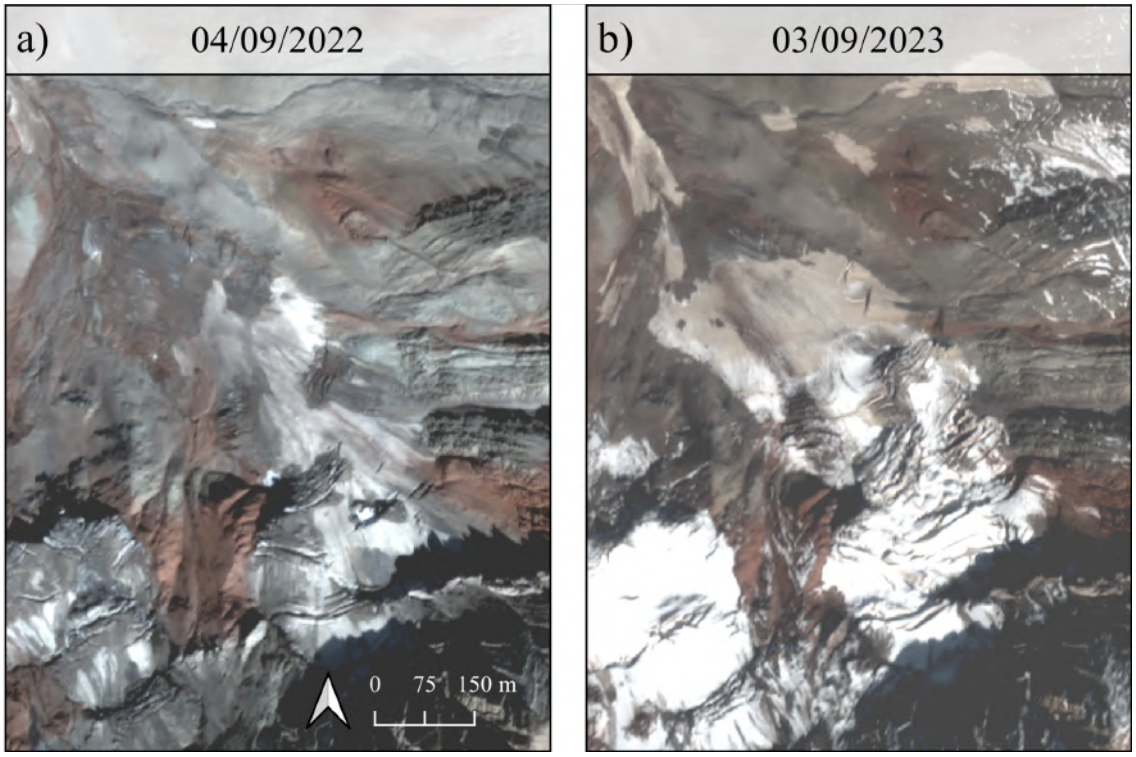

Figure A.4: Comparison of the surface of the glacier in the eastern subcatchment of Shuraki Kapali in the years 2022 **(a)** and 2023 **(b)**. In 2022, the glacier has only a few crevasses, whereas in 2023 large parts of the glacier are covered with crevasses. **(a, b)** Pléiades.

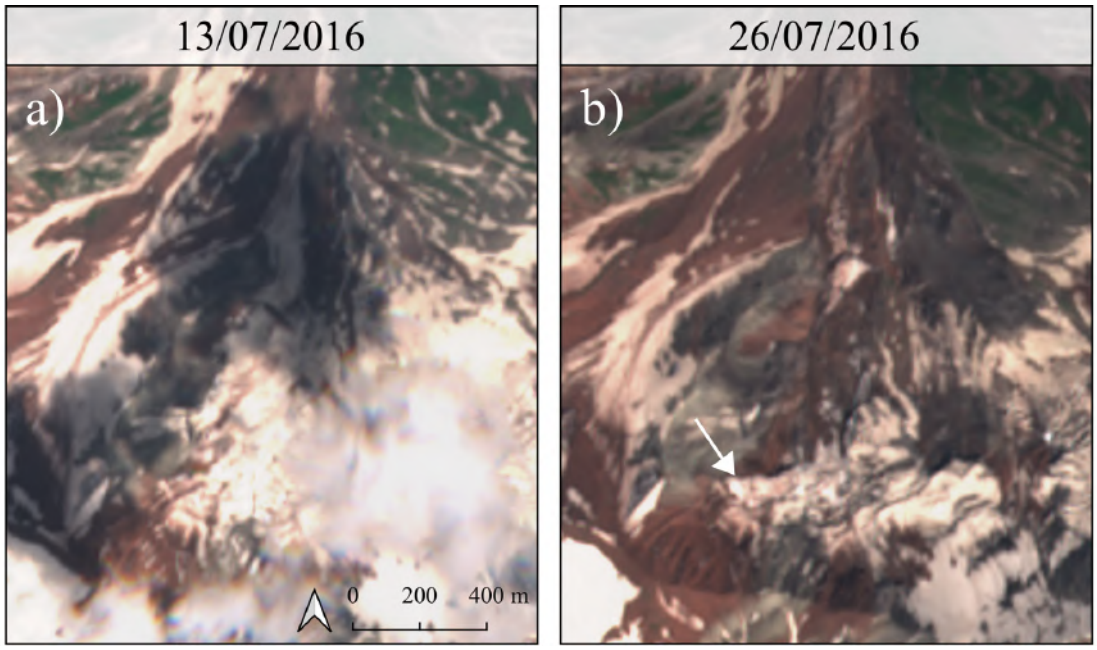

Figure A.5: The glacier in the central subcatchment before **(a)** and after **(b)** the detachment. The arrow points to the edge of the detachment. **(a)** Copernicus Sentinel data.

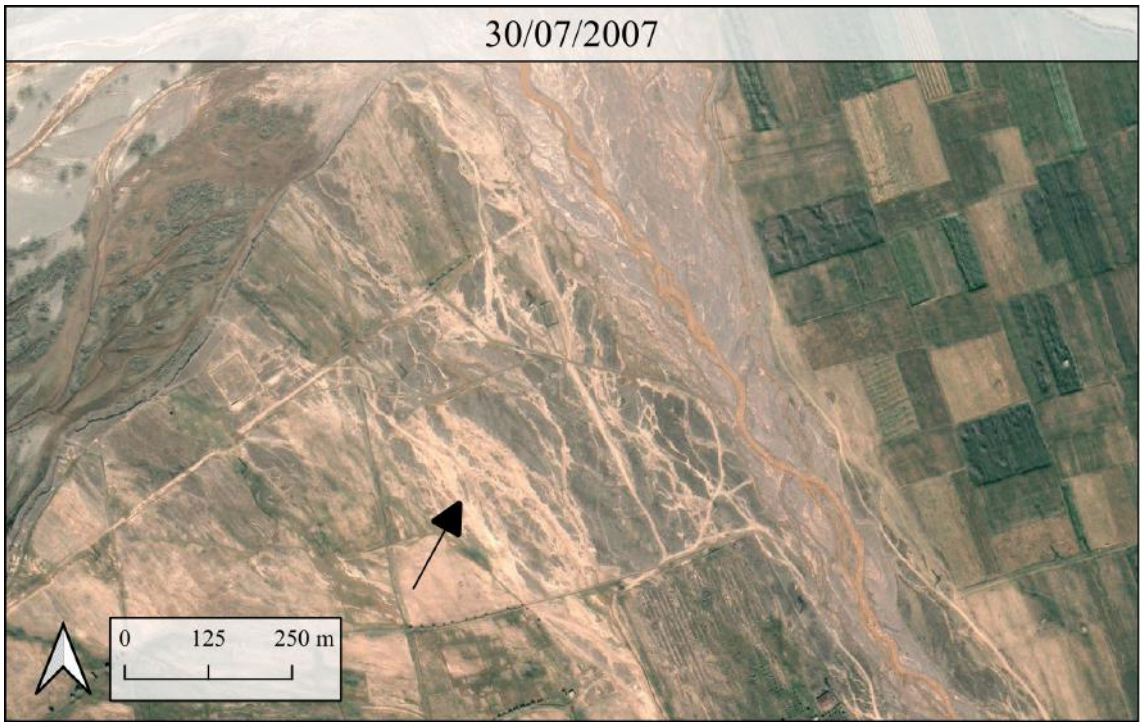

Figure A.6: The arrow points to one of the dried-out runoff channels that visible on the alluvial fan in the 30 September 2007 satellite image, indicating past flooding. © Google, Maxar Technologies.

Personal declaration: I hereby declare that the submitted thesis is the result of my own, independent work. All external sources are explicitly acknowledged in the thesis.